







## Kinematic analysis and palaeoseismology of the Edremit Fault Zone: evidence for past earthquakes in the southern branch of the North Anatolian Fault Zone, Biga Peninsula, NW Turkey

Hasan Sözbilir<sup>a,b,\*</sup> , Ökmen Sümer<sup>a</sup> , Çağlar Özkaymak<sup>c,d</sup> , Bora Uzel<sup>a</sup> , Tayfun Güler<sup>a</sup>  and Semih Eski<sup>b</sup> 

<sup>a</sup>Department of Geological Engineering, Dokuz Eylül University, TR-35160 İzmir, Turkey; <sup>b</sup>Earthquake Research and Application Center of Dokuz Eylül University, TR-35160 İzmir, Turkey; <sup>c</sup>Department of Geological Engineering, Afyon Kocatepe University, TR-03200 Afyon, Turkey; <sup>d</sup>Earthquake Research and Application Center of Afyon Kocatepe University, TR-03200 Afyon, Turkey

(Received 4 February 2016; final version received 4 April 2016)

The Edremit Fault Zone (EFZ) forms one of the southern segments of the North Anatolian Fault Zone (NAFZ) at the northern margin of the Edremit Gulf (Biga Peninsula, South Marmara Region, Turkey). Stratigraphic, structural and kinematic results indicate that basinward younging of the fault zone, in terms of a rolling-hinge mechanism, has resulted in at least three discrete Miocene to Holocene deformational phases: the oldest one (Phase 1) directly related to the inactive Kazdağ Detachment Fault, which was formed under N–S trending pure extension; Phase 2 is characterised by a strike-slip stress condition, probably related to the progression of the NAFZ towards the Edremit area in the Plio–Quaternary; and Phase 3 is represented by the high-angle normal faulting, which is directly interrelated with the last movement of the EFZ. Our palaeoseismic studies on the EFZ revealed the occurrence of three past surface rupture events; the first one occurred before 13178 BC, a penultimate event that may correspond to either the 160 AD or 253 AD historical earthquakes, and the youngest one can be associated with the 6 October 1944 earthquake ( $M_w = 6.8$ ). These palaeoseismic data indicate that there is no systematic earthquake recurrence period on the EFZ.

**Keywords:** Edremit Fault Zone; rolling-hinge mechanism; kinematic analysis; palaeoseismology; surface rupture

### 1. Introduction

The structural framework of the Marmara region is shaped by the western extension of the North Anatolian Fault Zone (NAFZ). There, the NAFZ is made up of at least two fault splays at its western termination, namely the northern and southern fault splays in the Marmara region (Figure 1(a)) (Barka, 1992; Barka & Kadinsky-Cade, 1988; Dewey & Şengör, 1979; Emre, Doğan, Özalp, & Yıldırım, 2011; Gürer, Kaymakçı, Çakır, & Özburan, 2003; Özalp, Emre, & Doğan, 2013; Şengör, 1979, Şengör et al., 2005, 2014). Towards the Biga Peninsula, the southern branch separates from the other by rightward step-overs. All of the above studies suggested that the Edremit Fault Zone (EFZ) forms the southwestern end of the southern branch of the NAFZ (Figure 1(b)). The EFZ was defined with different names by different researchers in previous studies, including the Küçükkuşu–Güre Fault by Siyako, Bürkan, and Okay (1989), the Behram Fault by Karacık and Yılmaz (1998), the Güre Fault by Okay and Satir (2000), the Edremit Fault by Yılmaz and Karacık (2001), the EFZ by Kaymakçı et al. (2007), the Edremit Fault by Cavazza, Okay, and Zattin (2009) and the EFZ by Emre and Doğan (2010). The formation mechanism and segmentation of the EFZ are explained by two views in the literature: (i) the EFZ is an active fault system with a combination of a low-angle normal fault (Kazdağ

Detachment Fault (KDF)) and high-angle synthetic/antithetic normal faults (Emre & Doğan, 2010; Emre, Doğan, & Yıldırım, 2012); and (ii) exhumation of the Kazdağ occurred in two phases, specifically the Oligo–Miocene (the low-angle KDF) and the Plio–Quaternary (high-angle normal and strike-slip faults cut and deformed the KDF) (Beccaletto & Steiner, 2005; Bonev, Beccaletto, Robyr, & Monié, 2009; Cavazza et al., 2009; Yaltrak, 2003, 2006; Yaltrak & Okay, 2004). According to the first view, the EFZ is divided into two subsegments, the Altınoluk and Zeytinli, considering changes in the structural features, geometry and characteristics of this fault zone (Emre & Doğan, 2010). The Altınoluk segment is 60-km long and consists of a main low-angle normal fault extending N80°E and zonal synthetic/antithetic high-angle normal faults, which developed in the hanging-wall of this main fault. At N30°E, the main trending Zeytinli segment forms the eastern part of the fault zone and is 15-km long; the segment is made up of a single structure that is the continuation of the main detachment fault of the Altınoluk segment. Kinematic indicators on slip planes, such as slickensides and riedels, indicate a right-lateral normal faulting with a minor strike-slip component in the western end and a strike-slip dominated oblique faulting at the eastern end; however, a number of studies specified that the major south-dipping low-angle detachment fault (KDF) observed

\*Corresponding author. Email: [hasan.sozbilir@deu.edu.tr](mailto:hasan.sozbilir@deu.edu.tr)

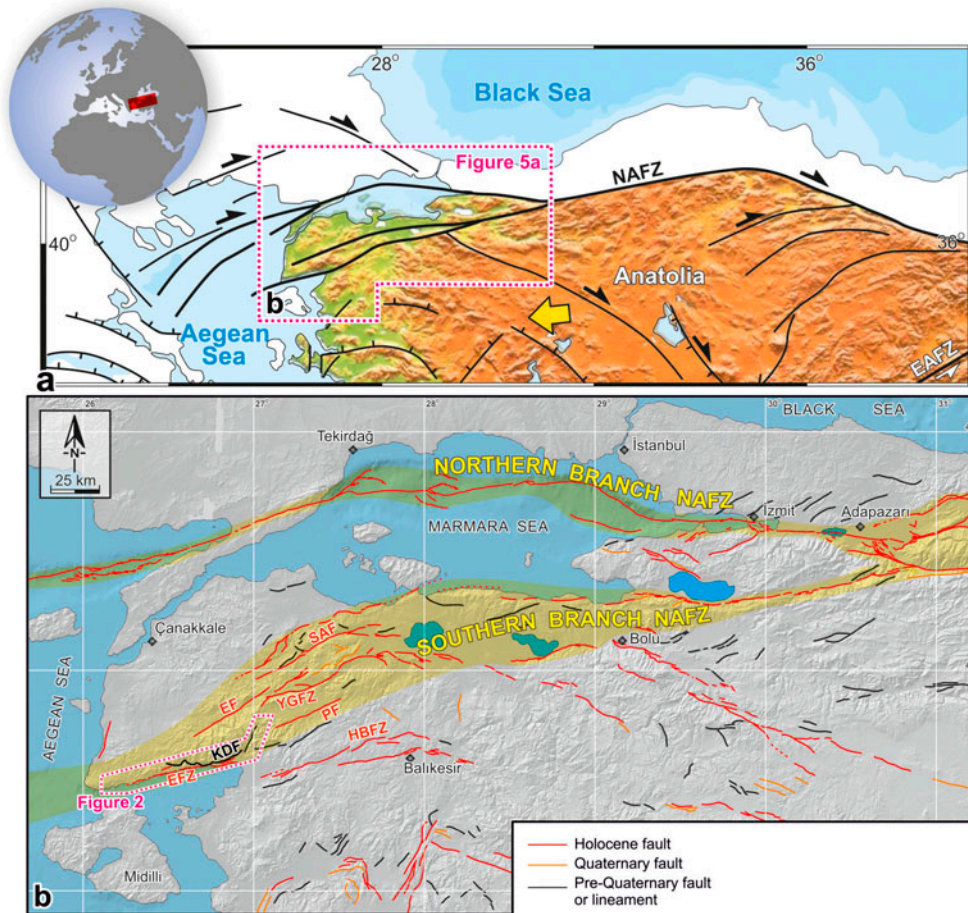


Figure 1. (a) Tectonic framework of the northern Anatolian block and surrounding regions (simplified from Barka, 1992; Şengör et al., 1985). (b) Active fault map of Marmara region (estimated branches of the NAFZ are shown in yellow shaded area). Major neotectonic structures compiled from General Directorate of Mineral Research And Exploration, Active fault map series of Turkey (Emre, 2010; Emre & Doğan, 2010; Emre, Doğan, Duman, & Özalp, 2011; Emre, Doğan, & Özalp, 2011; Emre et al., 2011; Emre, Duman, & Özalp, 2011a, 2011b, 2011c). The active faults in the Sea of Marmara were modified from (Armijo, Meyer, Navarro, King, & Barka, 2002; Cormier et al., 2006; Le Pichon et al., 2001). Yenice-Gönen Fault Zone (YGFZ), Sariköy Fault (SAF), Pazarköy Fault (PF), Evciler Fault (EF), Kazdağ Detachment Fault (KDF), Havran-Balıkesir Fault Zone (HBFZ) and Edremit Fault Zones (EFZ).

between the metamorphic rocks (footwall plate) and the volcano-sedimentary units (hanging-wall plate) is presently inactive, and this low-angle structure was cut and deformed by numerous younger east-west-trending, south-dipping high-angle normal faults (Beccalotto & Steiner, 2005; Bonev et al., 2009; Cavazza et al., 2009; Yaltrak, 2003, 2006; Yaltrak & Okay, 2004). One of them generated the 6 October 1944 Edremit earthquake ( $M_s = 6.8$ , Ambraseys, 1988;  $M_w = 6.7$ , Euro-Med Seismological Centre (EMSC)) that had a surface rupture of 38 km (Ambraseys & Jackson, 2000; Zimmermann, 1945), which was the largest earthquake that occurred on the EFZ in the instrumental period.

In this study, we performed palaeoseismological trench studies on the 1944 surface rupture in order to understand the seismic behaviour of the EFZ and whether the 1944 break followed a pre-existing fault or not. We also discussed the geodynamics evolution and kinematics features of the structural elements observed in the region during the detailed geological mapping of the

fault zone at a scale of 1/25000. Finally, we are the first to document the geologic, palaeoseismologic, and geoarcheologic evidence for the Holocene activity of the EFZ in terms of a rolling-hinge mechanism.

## 2. Tectono-stratigraphic features of the fault-belt rock units

In the northern part of the Edremit Bay, the geological units exposed along the EFZ can be mainly divided into two groups: the Kazdağ Metamorphics (footwall rock units) and the structurally overlying rock units that are composed of ophiolitic mélangé, metamorphic and volcano-sedimentary rocks (hanging-wall rock units) (Figure 2(a)).

### 2.1 Kazdağ metamorphics (footwall rock units)

The Kazdağ metamorphics were first defined as schist and gneiss units by Diller (1883). Then, Philippson

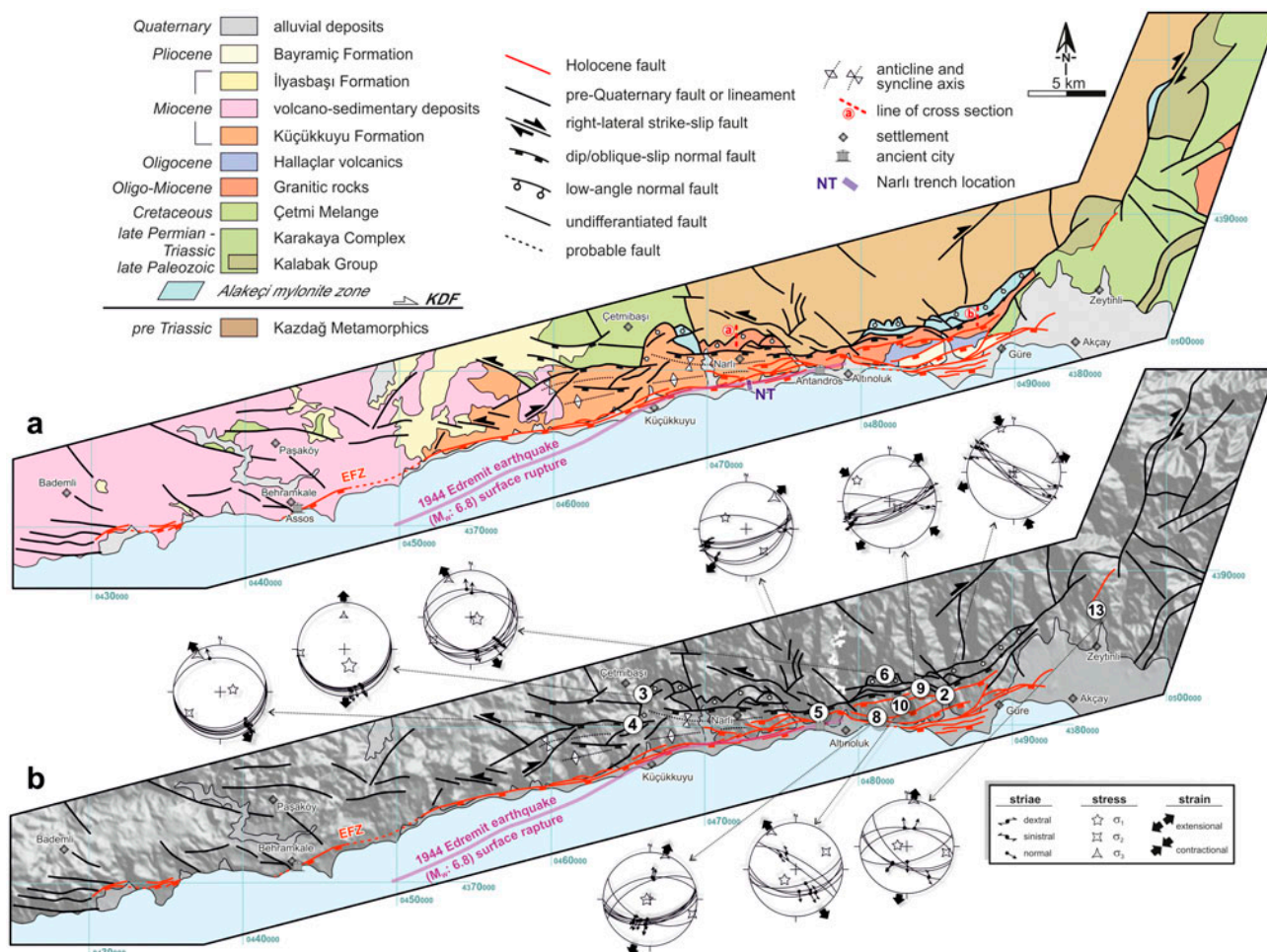


Figure 2. (a) Simplified geological map of the study area along the southern rim of Kazdağ mountain (modified from Emre and Doğan (2010), Duru, Pehlivan, Okay, Şentürk, & Kar (2012) and this study). 1944 surface rupture is completed from Altnok et al. (2012), Yaltrak (2006), and Zimmermann (1945); eyewitness recipes and field-based observations of this study; KDF:Kazdağ Detachment Fault, EFZ:Edremit Fault Zone. (b) Morphotectonic map of the study area showing distribution of palaeostress data sites, lower hemisphere equal-area projection of kinematic data and computed results of the principal stress axes.

(1910) and van der Kaaden (1959) mapped outcrops of these metamorphic rocks in the Kazdağ and the surrounding area. Schuiling (1959) indicated that the core part of the Kazdağ Massif has an N–S trending folding geometry and had undergone a high-temperature metamorphism before Hercynian. These marble- and metaclastic-dominated sequences were unroofed by KDF and formed the metamorphic core complex (Beccaleto & Steiner, 2005; Bonev et al., 2009; Cavazza et al., 2009; Lips, 1998; Okay & Satir, 2000; Yaltrak & Okay, 2004). The unit’s geological age has been the subject of many studies (Bingöl, 1971; Bonev et al., 2009; Cavazza et al., 2009; Duru, Pehlivan, Okay, Şentürk, & Kar, 2012; Erdoğan, Akay, Hasözbeç, Satir, & Siebel, 2013; Okay & Satir, 2000; Okay, Satir, & Siebel, 2006; Okay et al., 1996). When we synthesised these geological ages, which was performed via different radiometric dating methods, it was observed that the ages showed a wide range dispersion in terms of the geological intervals of 320–300 My, 250–216 My and 30–14 My. Additionally,

Okay and Satir (2000) and Bonev et al. (2009) pointed out that the last metamorphism occurred in the region at 5–6.9 Kb, 600–700 °C and a 20-km depth in the last phase of the Alpine orogeny in the late Oligocene–early Miocene.

## 2.2. Hanging-wall rock units

Duru et al. (2012) defined hanging-wall rock units as the Karakaya Complex and Çetmi Mélange. Bingöl, Akyürek, and Korkmazer (1973) described the Karakaya Complex of early Triassic low-grade metamorphosed clastic sediments covering the exotic limestone blocks with Permo-Carboniferous aged and metasiltite, spilitic basalt and diabasic rocks. Duru et al. (2012) expressed the age as late Permian (Culfiyen)–middle Triassic by using paleontologic records from exotic limestone blocks. They also stated that the Kalabak Group, which forms the basis of the Sakarya Zone in the Biga Peninsula, can be lithologically correlated with the units

described as lower the Karakaya Complex by Okay and Göncüoğlu (2004).

The northern and southern edges of the Kazdağ are characterised by cataclastic and mylonitic rocks. These rock assemblages were named the Alakeçilil mylonite zone by Okay (1987). Okay, Siyako, and Bürkan (1991) found that this zone is constituted mainly of mylonite gneiss and metaserpentine. The structurally overlying Çetmi Mélange was first defined by Okay et al. (1991) as olisthostromal. The matrix of the unit consists of fine-grained clastic rocks. Spilitic alkaline volcanic and pyroclastic rocks, eclogite slices and mostly recrystallised limestone are located as blocks within the unit. Based on stratigraphic and paleontologic studies (Beccaletto, Bartolini, Martini, Hochuli, & Kozur, 2005) performed within the unit, the age of the limestone blocks within the unit must be from the early Triassic–middle Albian and the matrix must be from the late Albian–Cenomanian.

The unconformably overlying Cenozoic rocks are made up of Kavlaklar granite, Hallaçlar volcanites, Küçükkuşu Formation, İlyasbaşı and Bayramiç formations, and alluvium.

The Kavlaklar granite was first named by Metzger (1994). Beccaletto (2003) and Beccaletto and Steiner (2005) pointed out that several small, elliptical-shaped granitoid bodies intruded the Çetmi Mélange and were clearly cut by the detachment fault, but they did not intrude on the Kazdağ Massif. However, field studies revealed that granitic rocks were separated from the metamorphic rocks by structurally low- and high-angle normal faults (Figure 3, cross-sections). Bingöl (1971) reported the age of the granitic rocks as  $25.3 \pm 3.0$ – $46.0 \pm 5.0$ – $70.5 \pm 8.0$  Ma using  $^{87}\text{Rb}/^{86}\text{Sr}$  and K/Ar methods. Beccaletto (2003) and Beccaletto and Steiner (2005) dated zircon grains between  $28.7 \pm .4$  and  $40.8 \pm 7.19$  Ma using the U–Th–Pb *in situ* ion-microprobe method, but the concordia  $^{238}\text{U}/^{206}\text{Pb}$  diagram for

zircons from the granodiorite indicates  $29.94 \pm .35$  Ma as the weighted average age.

Andesitic/basaltic lavas and pyroclastic rocks were defined under the name of Hallaçlar by Krushensky (1976), who described these rocks as being composed mainly of rhyodacite and minor labradorite, rhyodacite and trachyandesite. Krushensky, Akçay, and Karaege (1980) gave a K/Ar date of  $23.6 \pm .6$  Ma (J. D. Obradovich, U.S. Geol. Survey, written communication, 1971) on biotite from the lava flow of the Hallaçlar volcanites. Genç et al. (2012) reported K/Ar whole rock analysis of an andesitic sample as  $26.5 \pm 1.1$  Ma.

The Küçükkuşu Formation was identified by Saka (1979). According to Beccaletto (2003), this formation is represented by pebble stones, lava, and beige-coloured tuff intercalated lacustrine carbonates, bituminous shale containing mudstone, and volcanogenic sandstones. İnci (1984) suggested that this formation came from the early Miocene age, according to its sporomorph assemblage. Beccaletto and Steiner (2005) dated a biotite grain sample as  $34.4 \pm 1.2$  Ma from a tuffite of the upper member of the Küçükkuşu formation using the  $^{40}\text{Ar}/^{39}\text{Ar}$  method, but nevertheless they preferred to comment about this indicated age as given from a mobilised detritic material, which came from an older volcanic event that occurred in the Biga Peninsula. Cavazza et al. (2009) also suggested that apatite grains obtained from the tuffite sample, interbedded within the upper member of the formation, were  $16.8 \pm 2.6$  Ma as estimated by the apatite fission track method, which represents the depositional age of the upper part of the Küçükkuşu Formation.

The İlyasbaş Formation, outcropping almost 30 km<sup>2</sup> between the Çetmibaş and Paşaköy, was first named by Saka (1979). The formation is comprised predominately of limestone, clayey limestone and calcareous claystone, interbedded sandstone, and fine-grained conglomerates intercalated with pyroclastic airfall and flow deposits.

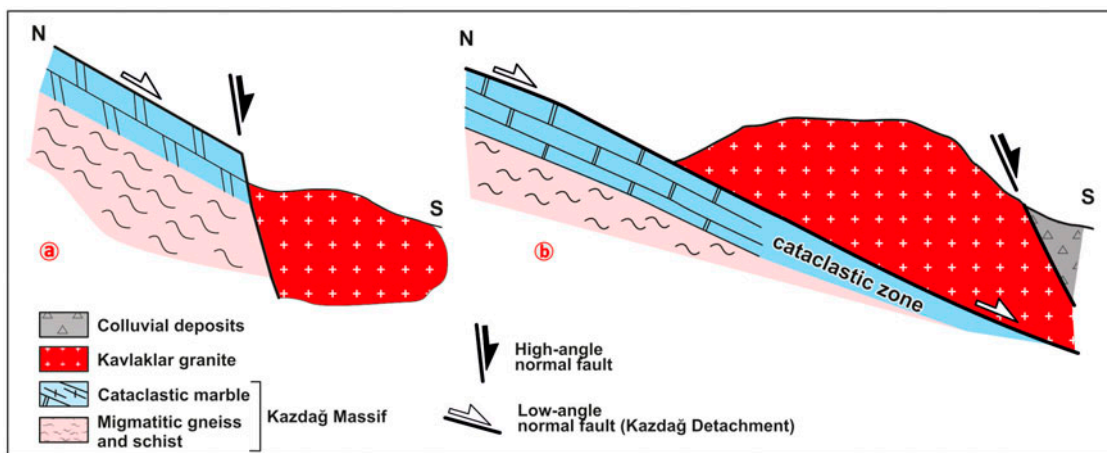


Figure 3. Field-based geological cross-sections (a) showing cross-cut relationship between low- and high-angle faults and (b) showing structural boundary between metamorphic rocks of the Kazdağ Massif and acidic plutonic rocks of the Kavlaklar granite (see Figure 2(a) for location of the sections).

The unit unconformably overlies the Küçükuyu Formation. Siyako et al. (1989) suggested that the relative age of the formation is from the late Miocene.

The Bayramiç Formation was firstly identified by Siyako et al. (1989) as small outcrops at the southern Kavaklar village. The unit, which extends to 3 km<sup>2</sup> through the fault zone, has a variable thickness of 50–150 m. The formation predominantly consists of conglomerates, blocky conglomerates, and moderately pebbly sandstone and mudstone. The formation rests unconformably on the basement rocks and it can be presumed to be from the Plio–Quaternary.

Quaternary sediments outcropping along the EFZ and northern edge of the Edremit Gulf consist of colluvial, alluvial fan, alluvial plain, beach, fluvial and fan-deltaic sediments. These unconsolidated/semi-consolidated sediments comprise unsorted crudely stratified gravel and cobble–pebble conglomerate, alternating with several coarse-graded angular and monomictic conglomerates.

### 3. Structural geology and kinematic analysis

In the study area, three different fault sets were recognised, which are associated with the Cenozoic deformation of the rock units, specifically the E–W-striking low-angle normal faults (KDF), NE–SW-striking oblique-slip faults (Conjugate Faults (CF)) and E–W-trending high-angle normal faults (EFZ) (Figure 2).

*Kazdağ Detachment Fault (KDF)*: It is a 1–3-km wide, 35-km long, approximately E–W-striking and gently S-dipping low-angle fault that mostly represents the structural contact between the Kazdağ Massif (foot-wall rocks) and the Kavaklar granite/Küçükuyu Formation (hanging-wall rocks). In the map view, the KDF displays the crescentic geometry that is characteristic of many detachment faults. Because of the rheological contrast between the footwall and hanging-wall units, the present-day morphology of the southern rim of the Kazdağ Massif is still controlled by the low-angle geometry of the KDF, with the gently seaward hill sloping at an angle of about 10–20° (Figure 4(a) and (c)). The KDF includes several well-developed fault planes that are comprised of breccias and mylonitic rocks (the Alakeçi Mylonite Zone) of the marbles or gneisses of the Kazdağ Massif. The fault planes include mostly SSW-trending slip lineations, indicating a south- to southeastward sense of movement (Figure 4(b) and (d)). Between the Çetmibaşı and Zeytinli villages, we measured more than 20 fault plane data points to analyse the kinematic behaviour of the KDF. According to the computed data, the major strike is around N80°E and the main dip is usually less than 25° to SE (plots 3, 4, and 6 in Figure 2(b)). Observed slickenlines ranged between 65° and 87°, characterising the dip-slip normal fault character. Additionally, field observations on footwall mylonitic rocks indicate a general top-to-the-south sense of shear, which is probably related to the exhumation of the metamorphic rocks of the Kazdağ Massif. The KDF

is cut and displaced by the other fault sets belonging to the NE–SW-striking CF and E–W-trending high-angle normal faults (Figure 3). Therefore, the KDF can be identified as not only seismically inactive, but also an older structure in the mapped area.

*Conjugate faults (CF)*: These structures were mapped mostly in the area between Çetmibaşı and Zeytinli as two different fault subsets that had NE–SW and NW–SE strikes (Figure 2). The length of these faults was measured up to 6 km. In the study area, the CF cut and displaced Miocene volcano-sedimentary units and older rocks. These second-order faults have well-preserved fault planes, striking between N50°W and N30°E with an average dip of 80° to the S, and their rakes are usually less than 20°. According to the collected kinematic data along these structures (see plot 2 in Figure 2(b)), NW-striking ones had a left-lateral strike slip character with a reverse component, while the NE-trending faults had a right-lateral strike slip motion. In particular, NW of Narlı village, a series of NW-trending strike-slip faults cut and left-laterally displaced the master faults of the KDF and also some stratigraphic contacts of the Miocene units. However, these CF were dissected by the E–W high-angle normal faults of the EFZ.

*Edremit Fault Zone (EFZ)*: The EFZ is the northern incipient bounding structure of the Edremit Gulf. It is an E–W-trending, range-front active normal-fault zone approximately 2–5-km wide and 75-km long (Figure 2). It bounds the Biga Peninsula to the south and consists of several fault sets lying between the Bademli and Edremit settlements (plots 5, 8, 9, 10 and 13 in Figure 2(b)). Between Bademli and Küçükuyu, the EFZ can be traced along the northern coast of the Edremit Gulf. It includes many fault segments striking between N80°W and N80°E, with an average dip of 70°SE. In this section, the EFZ not only cuts the Pliocene Bayramiç Formation, but also controls the actual shoreline of the Aegean Sea (Figure 2). Around Narlı, the EFZ has clear corrugations with variable-sized wavelengths, up to km-scale amplitude. Their map view shows a basinward-facing step-like fault pattern that is convex to the south. The general trend of the fault zone is measured approximately as E–W, and the average dip is observed around 65° to the S. Here, the EFZ cuts and elevates Miocene volcano-sedimentary rocks, while its southernmost segment separates Holocene alluvial deposits from older rocks. There are also many series of actively growing lateral alluvial fans aligned parallel to the fault. In this part of the fault zone, some northern segments striking N80°E, with an average dip of 56°SE, and rakes, changing between 70° NE and 75° NE, control the Holocene unconsolidated colluvial deposits (Figure 4(e) and (f)). Towards the east, where the eastern fault sets of the EFZ trend E–W to NE and enter Güre village, the EFZ includes several en-échélon arranged synthetic and anti-synthetic fault segments, dipping to the SE and NW, respectively (Figure 2). The observed fault planes strike around N70°E, dipping, on average, at 60°SE. Through the



Figure 4. Field photos of low- and high-angle normal faults. (a and c) low-angle detachment surface dipping towards the south, photos taken from Palamutluk and Değirmen hills, respectively. (b and d) close-up views of the dip-slip lineations with rakes of 80°–85° SE. (e) high-angle normal and its hanging wall colluvial deposits. (f) close-up views of the dip-slip lineations with rake of 75° SE.

village of Zeytinli, the fault cuts Holocene alluvial deposits, striking at N60°E, and manifests as an oblique-slip south-dipping normal fault with striations larger than 55°. In additionally, the fault zone shows a horsetail geometry, characterising the typical tip of a strike and/or oblique slip fault, in the map view. According to field observations, kinematic data, and morphological features (such as deflected valleys, vertically displaced Holocene terraces, and triangular facets), the EFZ can be identified as active and the youngest structure.

### 3.1. Paleostress analysis of fault-slip data

Palaeostress computation from fault slip data informs us not only about the orientation of the three principal stress axes, the maximum ( $\sigma_1$ ), intermediate ( $\sigma_2$ ) and minimum ( $\sigma_3$ ) principal stress axes, but also the ratio of the principal stress differences, also known as the shape ratio of the stress ellipsoid, formulated as  $\Phi = (\sigma_2 - \sigma_1) / (\sigma_3 - \sigma_1)$ . To do that, a number of graphical (e.g. Alexandrowski, 1986; Krantz, 1988) and numerical

palaeostress methods (e.g. Angelier, 1979, 1994; Armijo, Carey, & Cisternas, 1982; Delvaux & Sperner, 2003; Marrett & Allmendinger, 1990; Will & Powell, 1991; Yamaji, 2000; Yin & Ranalli, 1993; Žalohar & Vrabc, 2007) were developed for the computer-based inversion of structural data. Because of the robustness in multi-stage deformed areas (see Angelier et al., 1981; Brahim et al., 2002; Hippolyte & Mann, 2011; Kaymakçı, White, & van Dijk, 2000; Sperner et al., 2003; Vandycke & Bergerat, 2001), we used the Direct Inversion Method (INVD) of Angelier (1990) in this study; however, we refer to Angelier (1994) for a detailed review of the method and to Sperner and Zweigel (2010) and Hippolyte, Bergerat, Gordon, Bellier, and Espurt (2012) for data acquisition and separation techniques.

Briefly, the INVD is based on the reduced stress tensor concept and the estimation of the stress ellipsoid by the shape factor ( $\Phi$ ), which varies between 0 and 1. Thus, in areas where the stress ratio approximates 0 or 1, uni-axial stress conditions prevail and faults are not constrained in any direction. Otherwise, stress is tri-axial, all of the principal stress magnitudes are significantly different, the fault orientations tend to develop parallel to  $\sigma_2$  directions and the fault directions approximate to an Andersonian mechanism (Anderson, 1951). The stress regime is determined by the nature of the vertical ones: extensional when  $\sigma_1$  is vertical, strike-slip when  $\sigma_2$  is vertical and contractional when  $\sigma_3$  is vertical. Delvaux et al. (1997) suggested that the stress regimes also varied as functions of the stress ratio: radial extension ( $\sigma_1$  vertical,  $0 < \Phi < .25$ ), pure extension ( $\sigma_1$  vertical,  $.25 < \Phi < .75$ ), transtension ( $\sigma_1$  vertical,  $.75 < \Phi < 1$  or  $\sigma_2$  vertical,  $1 > \Phi > .75$ ), pure strike-slip ( $\sigma_2$  vertical,  $.75 > \Phi > .25$ ), transpression ( $\sigma_2$  vertical,  $.25 > \Phi > 0$  or  $\sigma_3$  vertical,  $0 < \Phi < .25$ ), pure contraction ( $\sigma_3$  vertical,  $.25 < \Phi < .75$ ) and radial contraction ( $\sigma_3$  vertical,  $.75 < \Phi < 1$ ).

During the inversion process, we used the allowable maximum misfit angle (ANG) and the acceptable maximum quality estimator value (RUP) (Angelier, 1994) to separate heterogeneous and incoherent data. The ANG (the maximum misfit angle between observed slip and computed shear stress direction) was taken as  $25^\circ$ . The RUP, which ranges from 0% (calculated shear stress parallel to actual striae with the same sense and maximum shear stress) to 200% (calculated shear stress maximum, parallel to actual striae but opposite in sense), was taken here as 50%. If fault slip data exceed these limits, they were separated from the data-set and then recomputed as a new tensor. Finally, combining qualitative observations and collected fault slip data in homogenous stations led us to obtain a picture of stress state related to regional tectonic events with various styles (extension or contraction), in terms of chronology and orientation.

### 3.2. Palaeostress reconstruction

We collected more than 60 fault-slip data points from 9 locations to construct the palaeostress orientation of the

southern rim of the Kazdağ region. Data for the Edremit area were collected from the KDF, the EFZ and CF that occurred between the KDF and EFZ (Figure 2(a)). The results of the palaeostress analyses are depicted in Figures 2(b) and Table 1. The chronology of the palaeostress regime was deduced mainly from the age of the youngest host rock in the outcrop. These overprinting relationships, together with cross-cutting relationships and stratigraphic information, were used to determine the various deformation phases and their succession in time. If no cross-cutting or overprinting relationships were encountered, the age of the host lithology and the similarity of the stress orientations/stress ratios to other sites were taken into account when the deformation phase was already precisely assigned (Hippolyte et al., 2012; Sperner & Zweigel, 2010). After processing fault-slip data, three different deformation phases can be separated, according to our results and the available kinematic data from the literature (Beccaletto & Steiner, 2005; Bonev et al., 2009). Phase 1, relating directly to the detachment fault, is characterised by a N–S directed pure extension and likely took place during the Miocene. This phase was followed by a second one (Phase 2) – its data were from the strike-slip motion of the EFZ, which is highlighted as the associated NE–SW trending extension and NW–SE trending contraction. This stress state was most probably related with the initiation of the NAFZ through the Edremit area. Although the formation of the NAFZ is still contradictory (Serravalian of Barka & Hancock, 1984; Dewey & Şengör, 1979; Şengör, 1979; Şengör, Görür, & Şaroğlu, 1985; or Pliocene of Barka & Kadinsky-Cade, 1988; Koçyiğit, 1988; Koçyiğit, Yılmaz, Adamia, & Kuloshvili, 2001), we assume the age of this deformation as during the Plio–Quaternary. The youngest stress state (Phase 3) is characterised by normal faulting along the EFZ. This deformation is associated with a NE–SW-striking extension.

Table 1. Characteristics of stress states used to reconstruct the stress regimes as illustrated in Figure 2(b).

Location	Principle stress axes (direction°/plunge°)			$\Phi$	#	ANG	RUP
	$\sigma_1$	$\sigma_2$	$\sigma_3$				
<i>Kazdağ Detachment Fault (KDF)</i>							
3	164/60	265/06	359/29	.144	6	13	22
4	079/67	236/21	329/08	.678	7	18	46
6	104/79	239/08	330/08	.316	8	15	28
<i>Conjugate Faults (CF)</i>							
2	344/03	208/86	074/02	.865	6	6	16
<i>Edremit Fault Zone (EFZ)</i>							
5	299/48	142/39	042/12	.758	7	21	45
8	266/85	109/05	019/02	.367	9	14	14
9	303/18	129/72	034/02	.716	8	12	32
10	227/63	060/26	327/05	.515	6	18	31
13	277/74	099/16	009/01	.583	6	24	35

Notes: #, Number of fault slip data;  $\Phi$ , ratio of stress magnitude. ANG and RUP are quality estimators. For detailed descriptions see Section 3.1. Palaeostress analysis of fault-slip data.

*Phase 1 – Miocene:* This phase is recognised at three stations (Figure 2(a) and Table 1). Data were collected from low-angle, normal-fault planes, which form the southern hill of Kazdağ High. The orientation of the horizontal principle stress was relatively consistent between stations, and it was oriented NNW–SSE to N–S (Figure 2(b)). The INVD technique calculated a near horizontal  $\sigma_3$ , trending approximately  $330^\circ$  with a  $8^\circ$  plunging, whereas the maximum principle stress axis ( $\sigma_1$ ) had a vertical attitude with an approximately  $70^\circ$  plunge. The main orientation of the  $\sigma_2$  was quite variable, with an approximately horizontal plunge ( $<20^\circ$ ). The calculated shape factors ( $\Phi$ ) ranged between .144 and .6678, suggesting that radial- to pure-extension was dominant during Phase 1. The age of this phase is overlaps with the formation of the Küçükuyu Formation and the exhumation of the Kazdağ Massif.

*Phase 2 – Plio–Quaternary:* The second deformational phase is characterised by strike-slip faulting that deformed both the Miocene units and the KDF. In this phase, the palaeostress orientations were obtained at three stations along the EFZ (Figure 2(b) and Table 1). The computed fault-slip measurements define a near horizontal  $\sigma_1$ , plunging about  $20^\circ$  with a  $300^\circ$  trend. The calculated minimum principle stress axis ( $\sigma_1$ ) also gently plunged ( $<12^\circ$ ), whereas the dip of  $\sigma_2$  varied between  $39^\circ$  and  $86^\circ$ . The main trend of  $\sigma_3$  was relatively consistent for all stations and in a range of  $34^\circ$ – $74^\circ$ . The computed shape factors used to estimate the stress state suggest that the Phase 2 structures formed in charge of the strike-slip regime ( $.716 < \Phi < .865$ ). These approximately E–W-trending strike-slip faults seem to form under an intense strike-slip tectonism affect, which is most probably associated with the continuation of the NAFZ through the study area.

*Phase 3 – Holocene:* This phase, evidenced by the youngest structures, indicates extensional deformation within the region. The orientation of the extensional strain axes varies from the NNW–SSE to NE–SW, which is characterised by high-angle normal faulting along the EFZ (Figure 2(b) and Table 1). However, having both step-like normal faults and shape factors ranging between .367 and .583 imply that Phase 3 is associated with pure extensional setting, considering the existence of active strike-slip faults in neighbouring areas, such as the Evciler Fault and Yenice–Gönen Fault Zones (YGFZs) in Figure 1, suggesting that the regional tectonics is mostly transtensional around the Biga Peninsula. The focal plane solutions of recent earthquakes also support a combination of extensional and strike-slip deformations (Figures 1 and 5). Structures of this youngest phase control the northern boundary of incipient Edremit Bay all along the coast line.

#### 4. Seismotectonics of the region

The Marmara region is one of the most important locations for researchers to pay attention to, especially the region's

historical and instrumental seismicity, considering the archaeological background of the area and the presence and efficiency of the NAFZ, which is one of the largest active strike-slip faults in the world. Also, the Marmara region is a densely populated and fast-developing part of Turkey; an important percentage of Turkey's industrial and communication facilities are concentrated over in the region roughly bounded by  $39.5\text{ N}$  to  $41.0\text{ N}$  and  $26.0\text{ E}$  to  $31.0\text{ E}$  (Figure 5(a)).

The Marmara block has different seismic characteristics from the rest of Anatolia and appears to act as a separate tectonic unit (Crampin & Evans, 1986). Accurate determination of focal depths using the joint hypocentre location techniques used by Jackson and Fitch (1979) and the modelling of the long-period body-waves by Eyidoğan and Jackson (1985) indicate that the major earthquakes in the region are not deeper than 10–15 km (Eyidoğan, 1988). These shallow earthquakes and their seismic magnitudes, scanned from many catalogues and researches (close to 500) with  $4 \leq M$  events that occurred in the Marmara region from 1900 to 2015, are illustrated in Figure 5(a). The NAFZ generated 15 major earthquakes within the last century. The total length of the surface rupture of these earthquakes occurred in excess of 1100 km (Özalp et al., 2013). Six of these 15 destructive earthquakes, including those in Düzce (1999) and Gökçeada (2014) with  $6.5 \leq M$ , occurred in the Marmara region and its surroundings. Additionally, the 1953 Yenice–Gönen earthquake stands out as one of the  $7 \leq M$  earthquakes that occurred in the southern branch during the instrumental period. The fault mechanism solutions of the major events, collected from many studies, indicate that the region was primarily shaped under the strike-slip deformation pattern (Figure 5(a)).

Ambraseys and Finkel (1991) reported that the total number of earthquakes for the period AD 1 to 1899 amounts to just under 600, and 38 described events are estimated to be relatively large shocks of magnitude  $7.0 \leq M$ , in the region; the estimated epicentre location of 59 historical earthquakes  $6.8 \leq M$  that affected and specifically damaged the region which were collected from Ambraseys and Finkel (1991), Ambraseys (2002), Shebalin, Karnik, and Hadzievski (1974), and Pınar and Lahn (1952), are also shown in Figure 5(a). The distribution of the both the historical and instrumental events indicate that the northern branch of the fault zone was more active than the southern one (Figure 5(a)). The last 2000 years of historical records reveal the existence of a similar earthquake cycle within the last century that occurred on the northern branch of the NAFZ (Ambraseys, 2002; Ambraseys & Finkel, 1991; Şengör et al., 2005).

Between 160 and 1898 AD, 30 earthquakes were reported at the western termination of the southern branch of the NAFZ, including the EFZ and the surrounding area in 18 locations.

Most historical earthquakes are focused around Lesvos Island (Figure 5(b)). The 11 October 1845



earthquake ( $I_0 = X$ ) was reported by Shebalin et al. (1974); the estimated location of the event is in the Edremit Gulf. This event was effective in a radius of 320 km, although the earthquake was felt more in Lesvos and the main damage occurred in the island (Papazachos & Papazachou, 1997). Another major earthquake was reported in the southern part of the Biga Peninsula and occurred on 7 March 1867 ( $M_w = 7.0$ , Soloviev, Solovieva, Go, Kim, & Shchetnikov, 2000;  $I_0 = X$  Shebalin et al., 1974;  $M = 7.0$ , Comninakis & Papazachos, 1982). The estimated location of this event is Lesvos Island, but it was felt in İstanbul, İzmir and even Athens; another earthquake caused great damage in the city of Mytilene, capital of Lesvos, and serious damage over a large area along the Turkish coasts (Altınok, Alpar, Yaltrak, Pınar, & Özer, 2012). This event destroyed more than 5750 houses, killed 550 people and injured 816 people (Papazachos & Papazachou, 1997). The smooth coastal section of Mytilene, which is located on the north-eastern part of the island, was flooded after the earthquake and covered by blurred mud; abnormal sea movements were observed at dawn the following day (Papazachos & Papazachou, 1997). Altınok et al. (2012) combined all these data with their own data and suggested that the 7 March 1867 earthquake should have created a tsunami in the Gulf of Edremit. In the Biga Peninsula, it is known that other significant earthquakes that affected the Hellespont region occurred in 155 AD and 160 AD. Although there is limited information about the 160 AD event in the literature, the magnitude of the earthquake was reported as  $M_s = 7.1$  by Ambraseys (2002). Likewise, Ambraseys and Finkel (1991) indicated that the 155 AD earthquake was a major earthquake that occurred in the provinces of Hellespont and Bithynia. They stated that Cyzicus (Erdek), together with other towns, was totally destroyed, Mytilini was damaged and the ground was extensively deformed in the interior of the Hellespont region. They also expressed that the shock was felt throughout Bithynia and caused great panic in Smyrna (İzmir) and Ephesus, and Cyzicus was restored with the financial assistance of Rome.

On the other hand, 19 earthquakes occurred ( $M > 3.5$ ) during the instrumental period in the EFZ and surrounding area. Two of them are mid-magnitude earthquakes, between 5 and 6. The 6 October 1944 earthquake ( $M_s = 6.8$ , Ambraseys, 1988;  $M_w = 6.7$ , EMSC) was the most powerful one within the instrumental period that affected Edremit city and its vicinity. The focal mechanism solutions of them indicate the normal faulting mechanism. These solutions are also compatible with the kinematic features of the EFZ. The main shock of the 1944 earthquake was felt in an area of approximately 250 km in diameter, which covers Akhisar, Manisa, Tekirdağ, Gonen and Lesvos island; during this earthquake, 73 people lost their lives, 275 people were injured and 2200 buildings were heavily damaged (Altınok et al., 2012). Zimmermann (1945) reported the surface rupture features in some localities, such as the cross-cut hill road going up to the village

of Adatepe, north of the Küçükkuyu. The expected fault rupture length associated with this event was calculated as 38 km by Ambraseys and Jackson (2000). Altınok et al. (2012) also reported that the tsunami waves were observed at some localities around the Gulf of Edremit, especially the southern part of the gulf and the Ayvalık coasts. Moreover, these researchers suggested the presence of an up to 2-m surface rupture in the vertical direction by using high-resolution shallow seismic reflections within the Edremit Gulf.

## 5. Palaeoseismology

### 5.1. Earthquake damages in the ancient city of the region

So far, in the areas covering Balıkesir and Çanakkale, a total of 95 pieces of ancient settlements had been determined in the Biga Peninsula, but 8 important ancient cities had been excavated: these are Troy, Apollon, Smintheus, Mabadi, Alexandria-Troas, and Assos in Çanakkale and Daskyleion, Antandros, Kyzikos, and Prokonnesos in Balıkesir. The ancient cities located near or on the EFZ are Assos, Lamponi, Antandros and Adramytteion. Two of them (Assos and Antandros) contain deformational structures that emerged during the earthquake(s).

#### 5.1.1. Assos

The ancient city was located on the northern edge and in the central part of the E–W trending coastline of the Edremit Gulf (Figure 5(b)). Serdaroğlu (1996) reported that the city was established by Leleges in 2000 BC. New researches carried out in the necropolis indicate the existence of a continuous settlement from the beginning of the seventh century BC until the end of the Roman period (Serdaroğlu, 1996). It is proposed that the Assos Theatre shifted and was largely destroyed by the earthquake(s) (Serdaroğlu, 1996). These damages were attributed to the 253 AD earthquake and/or the 6 October 1944 earthquake by Koçyiğit (2013) and Serdaroğlu (1996), respectively.

#### 5.1.2. Antandros

Antandros is located 4-km east of Altınoluk town (Edremit) in the southern flank of the Kazdağ Mountain (Figure 5(b)). The city was founded in the tenth century BC by the Pelasgians (Polat, 2002). Ongoing museum excavations in the necropolis, which had been used between the seventh century BC and second century AD, discovered many tombs that were placed on top of others two and three times using the slope angle, as well as cremation and direct burial grounds (Polat, 2008). The author states that the illegal excavations led to the discovery of a floor mosaic from the Roman period, and this situation resulted in systematic excavations that determine that it was a house that had frescoed walls

and covered mosaic floors dating from the first century AD (Dr Gürcan Polat, personal communication, 2013). We were carried out on the highlighted excavation area, which was located mainly near terrace houses to the east and the necropolis to the west (Figure 6(a)). These deformations observed in the necropolis area and terrace houses are shown in (Figure 6(b) and (c)), respectively. Especially in the necropolis area (Figure 7(a)), the cultural level differed in the presence of the tombs; however, the highest cultural level of the necropolis is dated to the second century (Polat, 2008). The deformations observed at the necropolis are generally characterised by fractures, cracks, collapses, sprains and backward distortions (Figure 6(b)). The deformations are concentrated in 3 points that include the boundary of the unearthed area and the systematic excavations. From west to east, these 3 points are, respectively, located in the northern border of the necropolis, in the middle section and in the east-south-east border of the excavation area. The northern margin of the necropolis is reposed on a boundary that lies between the Holocene alluvial coarse-clastic sediments and Miocene granitic rocks. In this area, one of the Roman tombs is also well preserved, but its northern wall is partly collapsed, distorted and back-tilted, with a concave geometry towards the south (Figure 7(b)). The

distorted geometry of the back-tilted wall seems to have occurred during a shaking event rather than a gravitational collapse. Both the orientation and location of this wall also intersect with an approximately E–W trending active fault, which extended between the Kavlaklar granite and the Holocene alluvial fan sediments.

The deformations in the middle part of the necropolis are observed on the sarcophagus belonging to the youngest culture level. The outward walls of the tombs were cracked, their corners were broken and the E–W trending longest sides exhibited a convex geometry towards the south (Figure 7(c)). In the easternmost point, an approximately E–W trending stone wall, which separated the tombs belonging to the older culture level, was also twisted towards the south in a convex geometry (Figure 7(d)). These deformations in the necropolis area extend along an approximately WNW–ESE trending zone (Figure 6(b)). Polat (2008) reported that the tombs that occurred in the different culture levels at Antandros Necropolis varied from the eighth century BC to the second century AD. The field data indicate that the deformations occurred on the sarcophagus dated starting from the lowest cultural level until the second century BC; as a result, one or more earthquakes affected the necropolis area after this date.

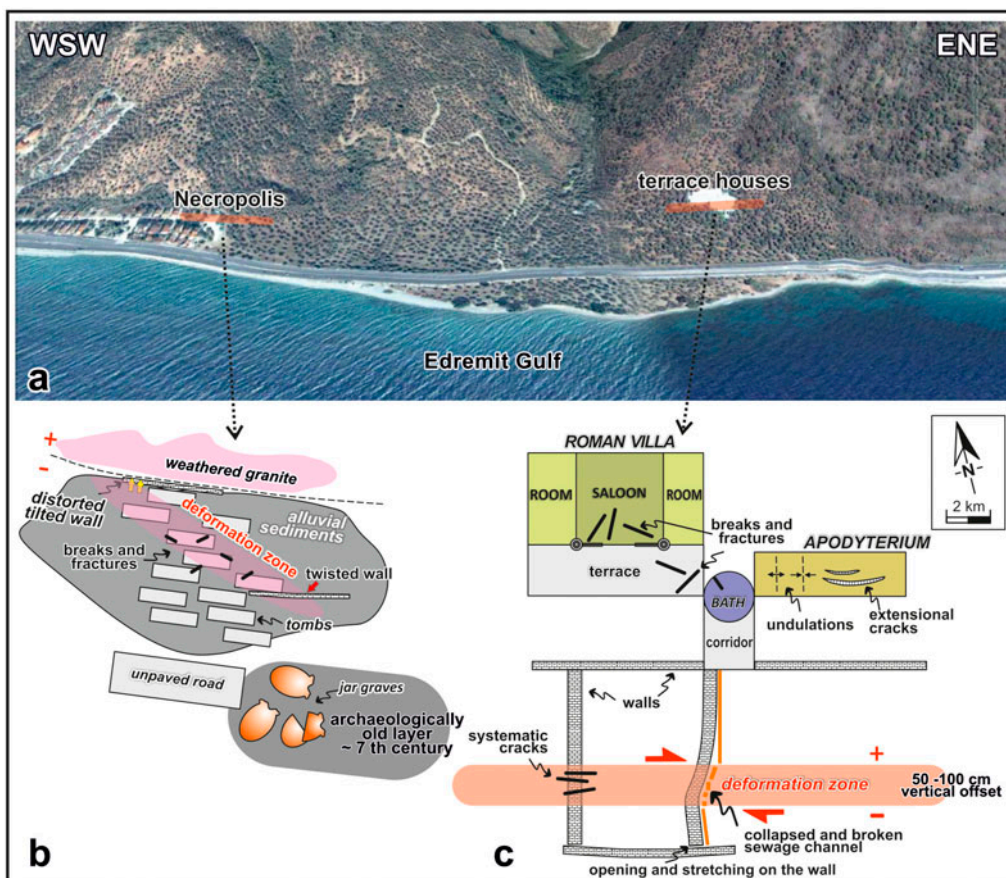


Figure 6. (a) Google earth image showing necropolis and terrace houses excavations areas in the Antandros. Sketch map of deformational structures in the area of necropolis (b) and terrace houses (c).



Figure 7. (a) Panoramic view of the necropolis, close up view of (b) distorted and back-tilted wall which is located in northwestern border of the necropolis area, (c) deformed sarcophagus at middle part of the necropolis, (d) twisted E–W trending stone wall at easternmost part of the necropolis. Dotted line and yellow arrows indicates rotation geometry, greens arrows show cracks and fractures.

Another key area with intense deformational structures is the terrace house, which is located in the eastern part of the excavation area. Two types of damage were observed at the terrace houses area: (a) damage related to co-seismic shaking and (b) rupture associated with surface break deformations. Shaking damage-related structures are concentrated on a Roman villa, which has been demonstrated in the recent excavations. These deformational structures are: fractures and cracks on a reception saloon and the terrace floor of the villa; broken corners and toppled walls of the house; geometrical diffractions on the Roman bath floor, which is located at the end of the corridor; breaks in the west-northwest section of the bath; a collapsed floor on the outside of the terrace; and extensional cracks and undulations, which are observed on the apodyterium floor (Figures 6(c) and 8(a)). The most distinctive evidence for the rupture associated with the surface break was observed on the N–S extending wall, which is located at the end of the

corridor in the southern part of the bath. The middle section of the wall was sprained by the right lateral shear effect (Figures 6(c), 8(b) and (c)). In addition, the sewage channel passing to the east of the wall was collapsed and broken due to the same buckling. Another parallel wall, which was located approximately 5-m west of this sprained wall, had E–W trending fractures and systematic cracks in the same direction (Figures 6(c) and 8(d)). Furthermore, this E–W-oriented deformation zone contained some vertical offsets, changing between 50 and 100 cm of displacement. These observations measured in two areas indicate that the deformational structures occurred and took place at the same elevation and orientation. This deformational zone and its trends at the Antandros are consistent with the E–W segments of the EFZ. Deformations occurred over these archaeologically dated structures, probably associated with one or more earthquakes that occurred on the EFZ after the first century BC.



Figure 8. (a) Extensional cracks and undulations observed on the floor (yellow arrows) of Apodyterium of the Roman villa (photo taken from [www.antandros.org](http://www.antandros.org)). (b and c) E–W directed dextral shear zone (red shaded area) on the ancient wall, dotted line indicates rotation geometry. (d) Systematic E–W trending cracks and fractures (yellow arrows) observed in the western wall. Persons for scale in all photos are 1.75-m long.

### 5.2. Trench studies

For the location of the trench, we considered both the compiled 1944 rupture information of some eyewitness and the results of the geological mapping studies. Some

eyewitnesses (Mr Veli Dayı, born in 1912 at Güre; Mr Mustafa Güder, born in 1928 at Narlı; Mr Hasan Turan, born in 1925 at Doyran; and Mr Mehmet Kavruk, born in 1929 at Küçükkuşu) showed us the exact

locations of the surface ruptures of the 1944 event. Moreover, they also reported that the rupture caused a hundreds-of-metres-long surface crack striking in an almost E–W direction at the south of Narlı village, which is also consistent with the our geologic mapping studies. Finally, the Narlı trench was dug perpendicular to the 1944 earthquake break on the EFZ to investigate whether the 1944 break followed a pre-existing fault (Figure 2(a)). The N–S-oriented Narlı trench is 27-m long and up to 4-m deep and wide. Both trench walls expose five units and the recent soil cover (Figures 9 and 10). The basement unit (unit 1) consists of the intercalations of light brown sandy silty mudstone (unit 1a), bluish, dark grey fine-grained sandy siltstone (unit 1b), yellowish, whitish mudstone and claystone (unit 1c) and dark brown organic-rich mudstone. It also includes randomly distributed lime nodules and channel-fill comprised of well-sorted, grey sandy conglomerates (unit 1d). The radiocarbon samples (samples NAR-WC-2 and NAR-WC-3) collected from the dark brown organic-rich levels of unit 1 yielded ages between 38912 and 36952 BC (Table 2), suggesting a late Pleistocene age of the unit that belonged to the Bayramiç Formation (Figure 9).

The V-shaped unit 2, consisting of gravelly, sandy mud, was interpreted as the crack fills, which are the products of the penultimate event. Units 1 and 2 are unconformably overlaid by unit 3, consisting of pinkish brown, gravelly, sandy mud.

The radiocarbon sample (sample NAR-EC-2, calibrated radiocarbon age data of the Narlı samples and their diagrams, which were sent to the Beta Analytic Radiocarbon Dating Laboratory, Miami, Florida/USA), collected from unit 3 on the east wall, yielded an age between 7180 and 7060 BC (Figure 10). Because of its vertical v-shaped plan view and their immature colluvial fabric, it is likely that unit 4 is crack fills, including greyish-brown, sandy, muddy gravels. Overlying the youngest unit, 5, is represented by light brown, gravelly, muddy, modern soil with an obtained age of  $100.2 \pm 03$  BP.

Based on the stratigraphical and sedimentological evidence and the analysis of the structural elements, three past surface rupture events were identified in the Narlı trench. The first event occurred before the deposition of unit 2 and after the deposition of unit 1. Hence, the age of unit 1 (samples NAR-WC-2 and NAR-WC-3) given above represents the lower boundary, while the

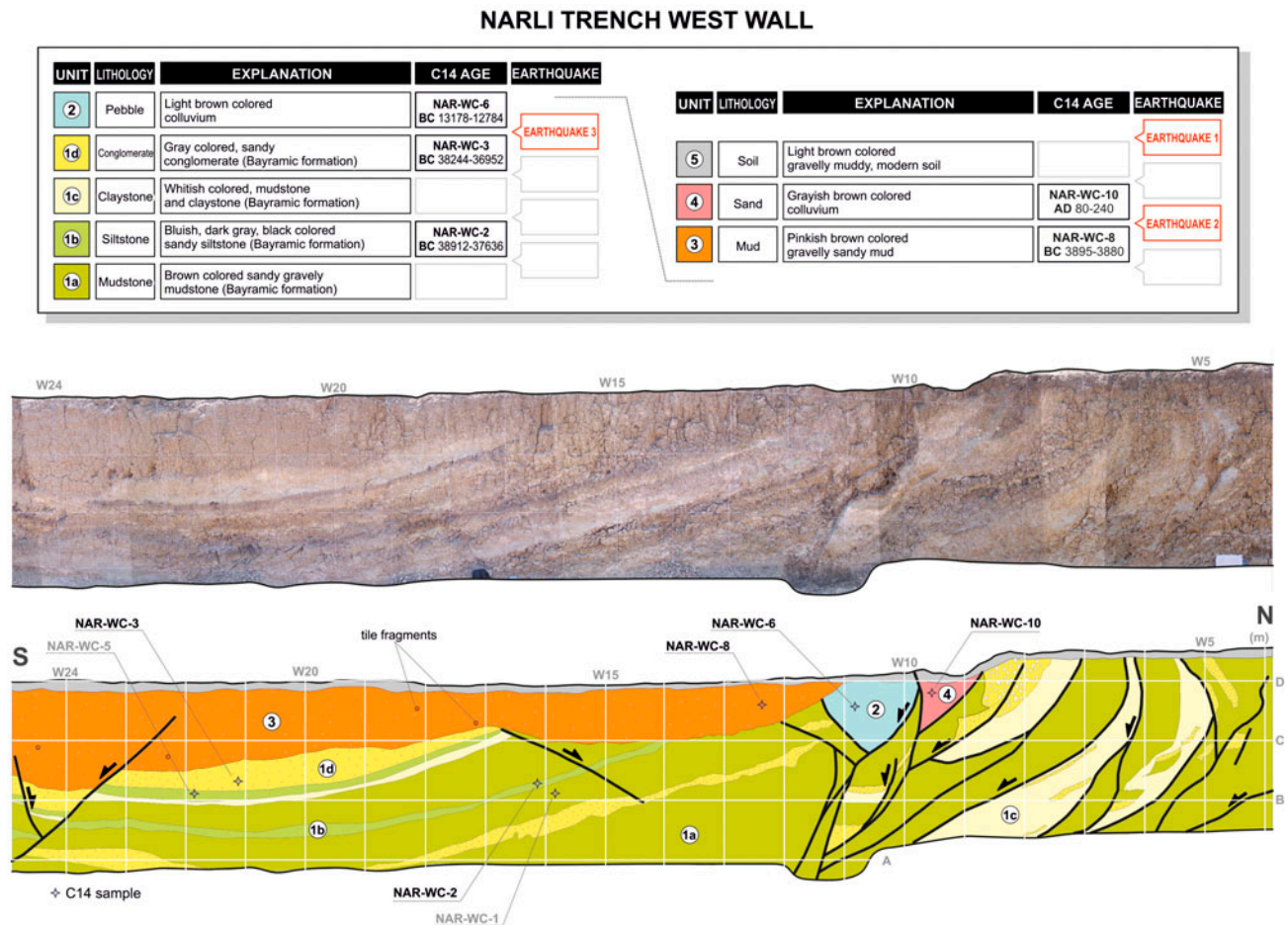


Figure 9. Photomosaic and palaeoseismological log of the west wall of Narlı trench. Note the past earthquakes and <sup>14</sup>C age data are also added to explanation of the units.

NARLI TRENCH EAST WALL

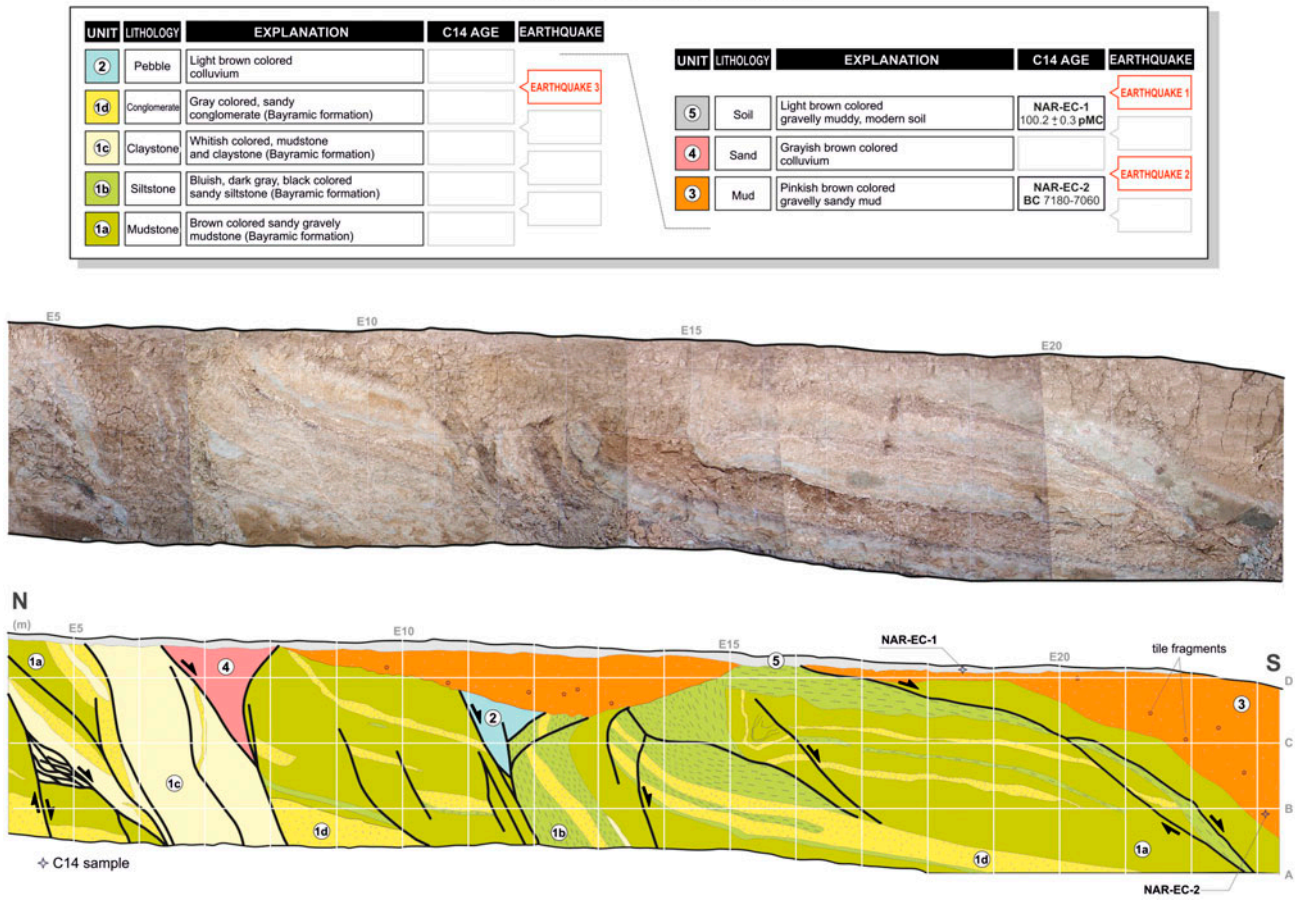


Figure 10. Photomosaic and palaeoseismological log of the east wall of Narlı trench. Note the past earthquakes and <sup>14</sup>C age data are also added to explanation of the units.

Table 2. Radiocarbon age data taken from the Narlı trench.

Trench name	Sample number	Lab. ID no.	Material type	Radiocarbon age (BP)	Two sigma range (AD or BC)
Narlı	NAR-WC-2	392555	Plant material	35600 ± 290	38912 BC–37636 AD
Narlı	NAR-WC-3	392556	Organic sediment	35040 ± 280	38244 BC–36952 BC
Narlı	NAR-WC-6	392558	Organic sediment	12590 ± 50	13178 BC–12784 BC
Narlı	NAR-WC-8	392560	Organic sediment	4980 ± 30	3895 BC–3880 BC
Narlı	NAR-WC-10	392562	Organic sediment	1850 ± 30	80 AD–240 AD
Narlı	NAR-EC-1	392552	Organic sediment	100.2 ± .3	1850 AD
Narlı	NAR-EC-2	392553	Organic sediment	8140 ± 30	7180 BC–7060 BC

upper boundary of the first event is defined according to the calibrated age of unit 2 (sample NAR-WC-6), which occurred between 13178 and 12784 BC. The second event, which deformed unit 3, also caused the crack fill that was filled by the deposits of unit 4. The unit 4 radiocarbon sample (sample NAR-WC-10) gave a calibrated age between 80 and 240 AD, suggesting that the penultimate event took place before about 160 ± 160 AD. The lower boundary of the second event is defined according to the calibrated age of unit 3 (sample NAR-WC-8), which occurred between 3895 and 3880 BC. The fault strand, which is a structural contact between

units 4 and 2, can be followed in recent soil (unit 5) and is probably related to the latest event (Figure 9).

5.2.1. Interpretation of palaeoseismological and geoarchaeological data

Three past surface rupture events were identified in the Narlı trench while digging on the Altınoluk segment of the EFZ. The Narlı trench shows that the source of the 1944 earthquake was the EFZ, and the 1944 break followed the pre-existing faults, which generated the penultimate event between 160 ± 160 AD and 3930 ± 50 BC

(Figure 11). The first event occurred before 13178 BC. The second event is likely to be associated with the historical earthquakes of 155 AD and/or 160 AD. The estimated locations, which were suggested by researchers, correspond to an area that is close to the Yenice–YGFZ. While 155 AD data are absent from the palaeoseismic studies performed by Kürçer et al. (2008), Belindir (2008) defined an event that occurred in 155 AD on the YGFZ. The 155 earthquake was reported in varied coordinates in different catalogues (Ambraseys & Finkel, 1991; Ambraseys & Jackson, 1998; Soysal, Sipahioğlu, Kolçak, & Altınok, 1981). When these catalogues are examined, it is obvious that the 155 and 160 earthquakes are different events. The coordinate distributions indicate that the 155 earthquake affected areas closer to the YGFZ, such as Bithynia, Cyzicus, Bandırma and Manyas. This information also increases the possibility that the 160 AD event occurred on the EFZ. The last event, the 1944 earthquake ( $M_w = 6.8$ ), caused a 35-

37-km surface rupture on the Altınoluk segment. The time after the last major earthquake for the Altınoluk fault segment is 72 years. Another remarkable detail is that the years between the 155 and 160 earthquakes seem too similar, with 9 years between the 1944 earthquake that occurred on the EFZ and the 1953 earthquake, which is the last event on the YGFZ. When we considered these earthquakes' locations, formation timings and magnitudes, it seems that the large earthquakes, which eventuated on the EFZ and were quite close to the YGFZ, triggered each other.

The palaeoseismological studies carried out in the northern branch of the NAFZ suggested that the estimated recurrence interval is 150–300 years for surface-ruptured large earthquakes (Hartleb, Dolan, Kozacı, Akyuz, & Seitz, 2006; Ikeda et al., 1991; Kozacı, Dolan, & Finkel, 2009; Kozacı, Dolan, Yönlü, & Hartleb, 2011; Özaksoy et al., 2010; Rockwell, Barka, Dawson, Akyuz, & Thorup, 2001; Rockwell et al., 2009), while

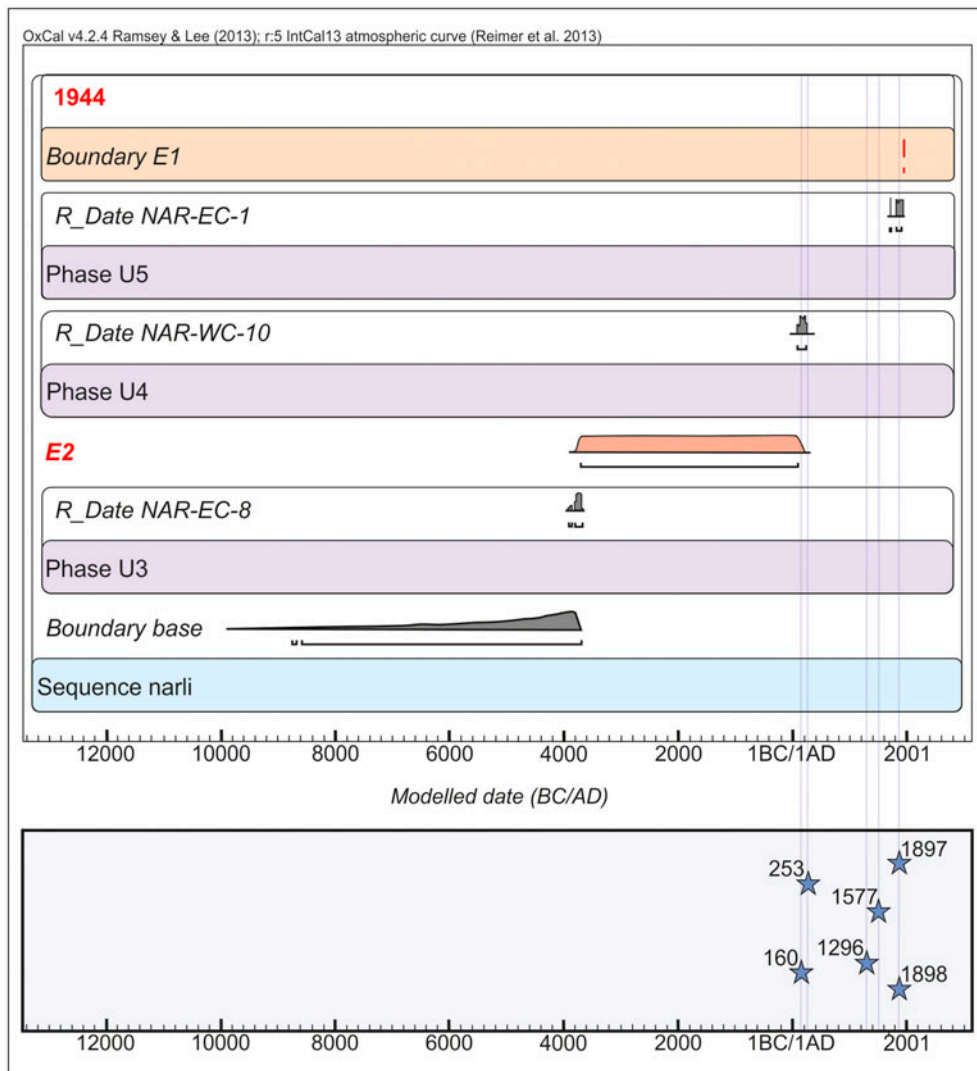


Figure 11. Probability distribution of calibrated  $^{14}\text{C}$  ages using OxCal v4.2.4 from Ramsey and Lee (2013) and r:5 IntCal13 atmospheric curve from Reimer et al. (2013) obtained from sequential radiocarbon dates collected from the Narlı trench walls. Blue stars indicate historical earthquakes.

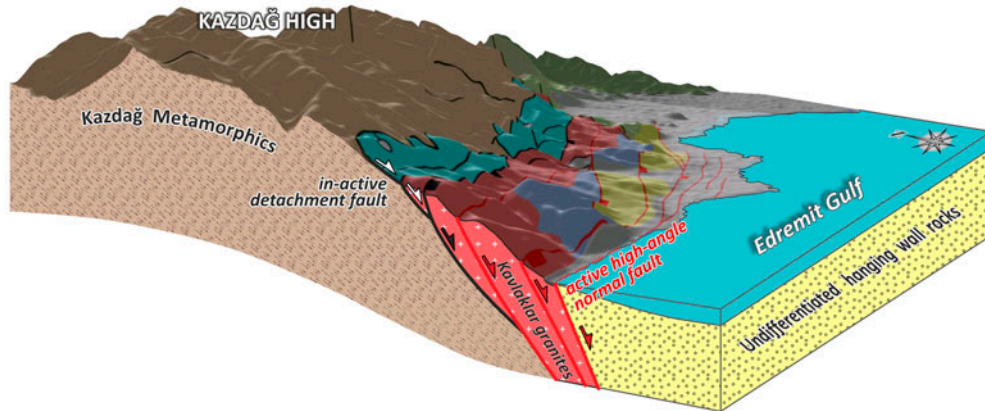


Figure 12. 3D block diagram showing structural relationships between low-angle and high-angle normal faults of Edremit Fault Zone in term of rolling-hinge mechanism. Note basinward migration of active faults. (see Figure 2 for explanations).

palaeoseismological studies on the southern branch are very limited, except for Yoshioka and Kuşçu (1994), Kürçer et al. (2008), Belindir (2008) and Özalp et al. (2013); however, Özalp et al. (2013) reported that the return period of the greater earthquakes that occurred on the southern branch was not regular, but these fault segments have the potential to produce earthquakes on the northern branch. Additionally, Belindir (2008) reported an earthquake recurrence interval on the YGFZ that ranged between 253 and 925 years. Kürçer et al. (2008) calculated the mean repetition period of the linear morphogenic earthquakes as  $660 \pm 160$  years on the same fault zone. According to the palaeoseismological data obtained from the Narlı trench, there was no systematic earthquake recurrence period of the EFZ, and this result is consistent with those found in other studies carried out in the southern branch of the NAFZ. Also, trench observations indicate that the faulting mechanism in the 1944 crack was used by the rupture that formed the previous events. At least three similar earthquakes occurred on the same rupture, which increases the probability that the next earthquake will occur on the same rupture that originated from the EFZ. Besides, the geometry of the deformational structures observed in the ancient city of Antandros, which are first revealed by this study, seems quite similar to the segment and kinematic features of the EFZ. The geometry, types and locations of these deformations, which were observed in the city and are dated between the eighth century BC and first century AD, indicate that they are related to one and/or more earthquakes that directly occurred on the EFZ after 1 AD. This *trouvaille* is also consistent with the palaeoseismological results obtained from the Narlı trench.

## 6. Discussion and conclusions

- The rock units outcropping around the fault zone are listed from old to young as follows: the

Karakaya Complex and Kalabak Group within the Sakarya Zone, the Kazdağ Massif, Çetmi Mélange, Kavaklar granites, Hallaçlar volcanics, Küçükuyu Formation, undifferentiated volcanic and volcanosedimentary rocks, İlyasbaşı and Bayramiç formations, and Quaternary alluvial, colluvial, fluvial, and deltaic deposits.

- The field observations and geological mapping studies indicate that the low-angle normal fault (Kazdağ Detachment) was cut and deformed by the high-angle normal faults of the EFZ, and rejuvenate towards the basin into the Edremit Bay. This mechanism shows significant similarities with the “rolling hinge” faulting mechanism in the literature (Figure 12). In this sense, the Kazdağı detachment, which was assessed within the EFZ, must be revised. In addition to this, the Zeytinli segment, which is described by Emre and Doğan (2010) as the eastern continuation of the main detachment fault, should also be reconsidered as an inactive fault class.
- Stratigraphic, structural and kinematic analyses indicate that the geodynamic evolution of the Edremit and its surroundings are traced by the three distinctive deformation phases from the Miocene to the present. The oldest one (Phase 1) is directly related to the activities of the KDF, which is represented by a N–S-trending pure extension. In contrast to Yılmaz and Karacık (2001) and Erdoğan et al. (2013), the results of Phase 1 clearly document that the tectonic setting during the Oligo–Miocene was a supra-detachment related to pure extension rather than contraction. Phase 2, which characterises a strike-slip stress condition, is probably related to the progression of the NAFZ towards the Edremit area during the Plio–Quaternary. The beginning age of this deformation phase has some controversies, and there are basically three different views: (i) as a result of the westward motion of Anatolia away from the

collision zone between the Arabian and Eurasian plates, the right lateral motion along the NAFZ is commenced by the Serravalian (Barka & Hancock, 1984; Dewey & Şengör, 1979; Şengör, 1979; Şengör et al., 1985); (ii) some researchers argued that the NAFZ was not initiated until the Pliocene (Barka & Kadinsky-Cade, 1988; Koçyiğit, 1988; Koçyiğit et al., 2001); and (iii) there are claims that the zone started to initiate in eastern Turkey during the late Miocene was propagated westwards, and did not reach the west until the Pliocene to form its recent shape and tectonic setting in the Marmara region (Barka, 1992; Okay, Demirbağ, Kurt, Okay, & Kuşçu, 1999; Suzanne et al., 1990). The last phase (Phase 3) is characterised by the high-angle normal faulting, which developed along the EFZ. This deformation is associated with a NNE–SSW-trending extension. Our field observations, such as the cross-cut relationship between the KDF and the EFZ, the youngest unit which was deformed in Phase 2 and the existence of post-dated strike-slip striations by normal ones indicate that the strike-slip faulting along the EFZ was active during the Plio–Quaternary. We therefore conclude that Edremit Bay may have started to develop in Phase 2, and then the modern shape of it took place in Phase 3, during the Holocene.

- In addition to the kinematic data collected from the fault planes of the EFZ, the focal mechanism solution of recent earthquakes, palaeoseismologic studies indicate that the 6 October 1944 earthquake occurred on the EFZ and caused an approximately E–W-trending, 35–40-km-long surface rupture that was nearly parallel to the shoreline.
- Three past surface ruptured events were identified in the Narlı trench. The first was before 13178 BC, the penultimate event may correspond to either the 160 AD or 253 AD historical earthquakes and the younger one can be associated with the 6 October 1944 earthquake ( $M_w = 6.8$ ). At least three similar earthquakes occurred on the same rupture, which increases the probability that the next earthquake will occur on the same rupture.

### Acknowledgement

We would like to gratefully thank to İdaköy Farm House employees and Azatoğlu Family for their warm hospitality during the field work. Also İskender Azatoğlu is gratefully thanked for fruitful discussions, guidance and wisdom about Kazdağ and surrounding area with 30 years of experience. We also acknowledge Antandros excavation director Dr Gürcan Polat in sharing fundamental information on the ancient city and archaeological excavations. Special thanks go to Narlı, Doyuran, Güre and Küçükkuşyü village headmen who guided us during our interviewing with eyewitness. We are also highly obliged to Mr Veli Dayı, Mr Mustafa Güder, Mr Hasan Turan and Mr Mehmet Kavruk for their contribution in the memory of the 1944

earthquake. We would like to thank sincerely to anonymous referees whose valuable comments and useful criticisms have greatly improved the manuscript. The paper was edited by American Manuscript Editors, an English language editing service.

### Disclosure statement

No potential conflict of interest was reported by the authors.

### Funding

This study is supported by National Earthquake Research Project No: UDAP-G-13-18 which has been realised in the frame of the Turkish Palaeoseismological Project (TURKPAP).

### ORCID

Hasan Sözbilir  <http://orcid.org/0000-0002-3777-4830>

Ökmen Sümer  <http://orcid.org/0000-0003-3168-8728>

Çağlar Özkaymak  <http://orcid.org/0000-0002-0377-1324>

Bora Uzel  <http://orcid.org/0000-0003-1703-5026>

Tayfun Güler  <http://orcid.org/0000-0002-8219-5539>

Semih Eski  <http://orcid.org/0000-0002-2526-2571>

### References

- Alexandrowski, P. (1986). Graphical determination of principal directions for slickenside lineation populations: An attempt modify Arthaud's method. *Journal of Structural Geology*, 7, 73–82.
- Altınok, Y., Alpar, B., Yaltrak, C., Pınar, A., & Özer, N. (2012). The earthquakes and related tsunamis of October 6, 1944 and March 7, 1867; NE Aegean Sea. *Natural Hazards*, 60, 3–25.
- Ambraseys, N. N. (1988). Engineering seismology: Part I. *Earthquake Engineering & Structural Dynamics*, 17, 1–105.
- Ambraseys, N. N. (2002). The seismic activity of the Marmara Sea region over the last 2000 years. *Bulletin of the Seismological Society of America*, 92, 1–18.
- Ambraseys, N. N., & Finkel, C. F. (1991). Long-term seismicity of Istanbul and of the Marmara Sea region. *Terra Motae*, 3, 527–539.
- Ambraseys, N. N., & Finkel, C. F. (2006). *Türkiye'de ve komşu bölgelerde sismik etkinlikler: Bir tarihsel inceleme, 1500–1800* [Seismic activity in Turkey and neighboring regions: A historical investigation, 1500–1800] (Academic serial 4). Ankara: TUBITAK Publications.
- Ambraseys, N. N., & Jackson, J. A. (1998). Faulting associated with historical and recent earthquakes in the Eastern Mediterranean region. *Geophysical Journal International*, 133, 390–406.
- Ambraseys, N. N., & Jackson, J. A. (2000). Seismicity of the Sea of Marmara (Turkey) since 1500. *Geophysical Journal International*, 141, F1–F6.
- Anderson, E. M. (1951). *The dynamics of faulting and dyke formation with applications to Britain*. Edinburgh: Oliver and Boyd.
- Angelier, J. (1979). Determination of the mean principal directions of stresses for a given fault population. *Tectonophysics*, 56, T17–T26.
- Angelier, J. (1990). Inversion of field data in fault tectonics to obtain the regional stress: III. A new rapid direct inversion method by analytical means. *Geophysical Journal International*, 103, 363–376.

- Angelier, J. (1994). Fault slip analysis paleostress reconstruction. In P. Hancock (Ed.), *Continental deformation* (pp. 101–120). Oxford: Pergamon.
- Angelier, J., Dumont, J. F., Karamanderesi, İ. H., Poisson, A., Şimşek, Ş., & Uysal, Ş. (1981). Analyses of fault mechanisms and expansion of southwestern Anatolia since the Late Miocene. *Tectonophysics*, 75, 11–19.
- Armijo, R., Carey, E., & Cisternas, A. (1982). The inverse problem in microtectonics and the separation of tectonic phases. *Tectonophysics*, 82, 145–160.
- Armijo, R., Meyer, B., Navarro, S., King, G., & Barka, A. (2002). Asymmetric slip partitioning in the Sea of Marmara pull-apart: A clue to propagation processes of the North Anatolian Fault. *Terra Nova*, 14, 80–86.
- Barka, A. A. (1992). The North Anatolian Fault Zone. *Annales Tectonicae*, 6, 164–195.
- Barka, A. A., & Hancock, P. L. (1984). *Neotectonic deformation patterns in the convex-northwards arc of the North Anatolian Fault Zone* (Vol. 17, pp. 763–774). London: The Geological Society, Special Publications.
- Barka, A. A., & Kadinsky-Cade, K. (1988). Strike-slip fault geometry in Turkey and its influence on earthquake activity. *Tectonics*, 7, 663–684.
- Beccaletto, L. (2003). *Geology, correlations and geodynamic evolution of the Biga Peninsula (NW Turkey)* (PhD thesis, p. 187). l'Université de Lausanne.
- Beccaletto, L., Bartolini, A. C., Martini, R., Hochuli, P. A., & Kozur, H. (2005). Biostratigraphic data from the Çetmi Melange, northwest Turkey: Palaeogeographic and tectonic implications. *Palaeogeography, Palaeoclimatology, Palaeoecology*, 221, 215–244.
- Beccaletto, L., & Steiner, C. (2005). Evidence of two-stage extensional tectonics from the northern edge of the Edremit Graben (NW Turkey). *Geodinamica Acta*, 18, 225–239.
- Belindir, F. (2008). *Yenice-Gönen fay zonunun Neotektonik özellikleri ve paleosismolojisi* [Neotectonic characteristics and paleoseismology of the Yenice-Gönen Fault Zone, NW Anatolia, Turkey] (PhD thesis, p. 293). Hacettepe Üniversitesi, Ankara (in Turkish with English Summary).
- Bingöl, E. (1971). Fiziksel (radyometrik, radyojenik) yaş tayini metodlarını sınıflama denemesi ve Rb-Sr ve K-A metodlarının Kazdağ'da bir uygulaması [The classification trying of physical age determination and an application of Rb-Sr, K-A methods in Kazdağ]. *Bulletin of the Geological Society of Turkey*, 14(1), 1–16 (in Turkish).
- Bingöl, E., Akyürek, B., & Korkmaz, B. (1973). Biga Yarımadası'nın jeolojisi ve Karakaya formasyonunun bazı özellikleri [The geology of Biga Peninsula and several features of Karakaya formation]. In *Cumhuriyet'in 50. Yılı Yerbilimleri Kongresi Tebliğler Dergisi*. General Directorate of Mineral Research and Exploration (MTA) Bulletin (pp. 70–76), Ankara (in Turkish).
- Boğaziçi University Kandilli Observatory and Earthquake Research Institute (KOERI). Retrieved from [www.koeri.boun.edu.tr/scripts/lst4.asp](http://www.koeri.boun.edu.tr/scripts/lst4.asp)
- Bonev, N., Beccaletto, L., Robyr, M., & Monié, P. (2009). Metamorphic and age constraints on the Alakeçi shear zone: Implications for the extensional exhumation history of the northern Kazdağ Massif, NW Turkey. *Lithos*, 113, 331–345.
- Brahim, L. A., Chotin, P., Hinaj, S., Abdelouafi, A., El Adraoui, A., Nakcha, C., ... Tabyaoui, H. (2002). Paleostress evolution in the Moroccan African margin from Triassic to present. *Tectonophysics*, 357, 187–205.
- Calvi, V. S. (1941). *Erdbebenkatalog der Turkei und Einiger Benaehbarter Gebiete* [Earthquake catalogue Turkey and some neighboring areas]. (Unpublished Report No. 276). Ankara: General Directorate of Mineral Research and Exploration (MTA).
- Camtez, N., & Toksöz, M. N. (1971). Focal mechanism and source depth of earthquakes from body- and surface-wave data. *Bulletin of Seismological Society of America*, 61, 1369–1379.
- Cavazza, W., Okay, A. I., & Zattin, M. (2009). Rapid early-middle Miocene exhumation of the Kazdağ Massif (western Anatolia). *International Journal of Earth Sciences*, 98, 1935–1947.
- Cominakakis, P. E., & Papazachos, B. C. (1982). *A catalogue of historical earthquakes in Greece and the surrounding area for the period 479 B.C.–1900 A.D.* University of Thessaloniki Publications, No. 5, 24 pp.
- Cormier, M. H., Seeber, L., McHugh, C. M. G., Polonia, A., Çağatay, M. N., Emre, Ö., ... Newman, K. R. (2006). North Anatolian fault in the Gulf of Izmit (Turkey): Rapid vertical motion in response to minor bends of a nonvertical continental transform. *Journal of Geophysical Research*, 111, 1–25.
- Crampin, S., & Evans, R. (1986). Neotectonics of the Marmara Sea region of Turkey. *Journal of the Geological Society*, 143, 343–348.
- Delvaux, D., Moeys, R., Stapel, G., Petit, C., Levi, K., Miroshnichenko, A., ... San'kov, V. (1997). Paleostress reconstructions and geodynamics of the Baikal region, Central Asia, Part 2. Cenozoic rifting. *Tectonophysics*, 282(1–4), 1–38.
- Delvaux, D., & Sperner, B. (2003). Stress tensor inversion from fault kinematic indicators and focal mechanism data: The TENSOR program. In D. Nieuwland (Ed.), *New insights into structural interpretation and modelling* (pp. 75–100). London: Geological Society Special Publications 212.
- Dewey, J. F., & Şengör, A. M. C. (1979). Aegean and surrounding regions: Complex multiplate and continuum tectonics in a convergent zone. *Geological Society of America Bulletin*, 90, 84–92.
- Diller, J. S. (1883). Notes of the geology of the Troad, A brief summary of the results derived from observations made in connexion with the Assos (U.S) expedition. *The Quarterly Journal of the Geological Society of London*, 2, 255–258.
- Duru, M., Pehlivan, Ş., Okay, A. İ., Şentürk, Y., & Kar, H. (2012). Biga Yarımadası'nın Tersiyer öncesi jeolojisi [Pre-Tertiary geology of Biga Peninsula]. In E. Yüzer & G. Tunay (Eds.), *Biga Yarımadası'nın Genel ve Ekonomik Jeolojisi* [General and Economic Geology of Biga Peninsula] Special series, 28 (pp. 7–74). MTA: Ankara (in Turkish).
- Emre, Ö. (2010). *1:250,000 Scale active fault map series of Turkey Çanakkale (NK 35-10b) Quadrangle* (Serial number: 1). Ankara: General Directorate of Mineral Research and Exploration (MTA).
- Emre, Ö., & Doğan, A. (2010). *1:250,000 Scale active fault map series of Turkey Ayvalık (NJ 35-2) Quadrangle* (Serial number: 4). Ankara: General Directorate of Mineral Research and Exploration (MTA).
- Emre, Ö., Doğan, A., Duman, T. Y., & Özalp, S. (2011). *1:250,000 Scale active fault map series of Turkey, Bursa (NK 35-12) quadrangle* (Serial number: 9). Ankara: General Directorate of Mineral Research and Exploration (MTA).
- Emre, Ö., Doğan, A., & Özalp, S. (2011). *1:250,000 Scale active fault map series of Turkey Balıkesir (NJ 35-3) quadrangle* (Serial number: 4). Ankara: General Directorate of Mineral Research and Exploration (MTA).
- Emre, Ö., Doğan, A., Özalp, S., & Yıldırım, C. (2011). *1:250,000 Scale active fault map series of Turkey Bandırma (NK 35-11b) quadrangle* (Serial number: 3). Ankara: General Directorate of Mineral Research and Exploration (MTA).

- Emre, Ö., Doğan, A., & Yıldırım, C. (2012). Biga Yarımadası'nın diri fayları ve deprem potansiyeli [The active faults of Biga Peninsula and its earthquake potential]. In *Biga Yarımadası'nın Genel ve Ekonomik Jeolojisi, Özel yayın serisi* (Vol. 28, pp. 163–198). Ankara: MTA.
- Emre, Ö., Duman, T. Y., & Özalp, S. (2011a). *1:250,000 Scale active fault map series of Turkey Adapazarı (NK 36-13) quadrangle* (Serial number: 14). Ankara: General Directorate of Mineral Research and Exploration (MTA).
- Emre, Ö., Duman, T. Y., & Özalp, S. (2011b). *1:250,000 Scale active fault map series of Turkey Eskişehir (NJ 36-1) quadrangle* (Serial number: 15). Ankara: General Directorate of Mineral Research and Exploration (MTA).
- Emre, Ö., Duman, T. Y., & Özalp, S. (2011c). *1:250,000 Scale active fault map series of Turkey Kütahya (NJ 35-4) quadrangle* (Serial number: 10). Ankara: General Directorate of Mineral Research and Exploration (MTA).
- Erdogan, B., Akay, E., Hasözbeke, A., Satır, M., & Siebel, W. (2013). Stratigraphy and tectonic evolution of the Kazdağı Massif (NW Anatolia) based on field studies and radiometric ages. *International Geology Review*, 55, 2060–2082.
- Ergin, K., Güçlü, U., & Uz, Z. (1967). *A catalog of earthquakes for Turkey and surrounding area (11 A.D. to 1964 A.D.)* (Technical Report No. 24). Istanbul Technical University, Faculty of Mines, Institute of Physics of the Earth.
- Euro-Med Seismological Centre (EMSC). Retrieved from <http://www.emsc-csem.org>
- Eyidoğan, H. (1988). Rates of crustal deformation in western Turkey as deduced from major earthquakes. *Tectonophysics*, 148, 83–92.
- Eyidoğan, H., & Jackson, J. (1985). A seismological study of normal faulting in the Demirci, Alaşehir and Gediz earthquakes of 1969–1970 in western Turkey: implications for the nature and geometry of deformation in the continental crust. *Geophysical Journal International*, 81, 569–607.
- Genç, Ş. C., Dönmez, M., Akçay, A. E., Altunkaynak, Ş., Eyüboğlu, Y., & Ilgar, Y. (2012). Biga Yarımadası Tersiyer volkanizmasının stratigrafik, petrografik ve kimyasal özellikleri [The stratigraphic, petrographic and chemical features of Biga Peninsula Tertiary volcanism]. In E. Yüzer & G. Tunay (Eds.), *Biga Yarımadası'nın Genel ve Ekonomik Jeolojisi* [General and Economic Geology of Biga Peninsula] *Special series*, (Vol. 28, pp. 122–162). MTA: Ankara (in Turkish).
- Gürer, Ö. F., Kaymakçı, N., Çakır, Ş., & Özbüran, M. (2003). Neotectonics of the southeast Marmara region, NW Anatolia, Turkey. *Journal of Asian Earth Sciences*, 21, 1041–1051.
- Hartleb, R. D., Dolan, J. F., Kozacı, O., Akyuz, H. S., & Seitz, G. G. (2006). A 2500-yr-long paleoseismologic record of large, infrequent earthquakes on the North Anatolian fault at Cukurcimen, Turkey. *Geological Society of America Bulletin*, 118, 823–840.
- Hippolyte, J. C., Bergerat, F., Gordon, M. B., Bellier, O., & Espurt, N. (2012). Keys and pitfalls in mesoscale fault analysis and paleostress reconstructions, the use of Angelier's methods. *Tectonophysics*, 581, 144–162.
- Hippolyte, J. C., & Mann, P. (2011). Neogene–quaternary tectonic evolution of the Leeward Antilles islands (Aruba, Bonaire, Curaçao) from fault kinematic analysis. *Marine and Petroleum Geology*, 28, 259–277.
- HRV. Harvard Centroid–Moment Tensor Project CMT, Harvard University, MA, USA (1977–2015). Retrieved from <http://www.globalcmt.org/CMTsearch.html>
- Ikeda, Y., Suzuki, Y., Herece, E., Şaroğlu, F., Işıkara, A. M., & Honkura, Y. (1991). Geological evidence for the last two faulting events on the North Anatolian Fault Zone in the Mudurnu Valley, western Turkey. *Tectonophysics*, 193, 335–345.
- İnci, U. (1984). Demirci ve Burhaniye Bitümlü Şeyllerinin Stratigrafisi ve Organik Özellikleri [The stratigraphy and organic features of Demirci and Burhaniye bituminous shales]. *Bulletin of the Geological Society of Turkey*, 5, 27–40.
- International Seismological Centre (ISC). Thatcham, UK. Retrieved from <http://www.isc.ac.uk/Bull>
- Jackson, J., & Fitch, T. J. (1979). Seismotectonic implications of relocated aftershock sequences in Iran and Turkey. *Geophysical Journal International*, 57(1), 209–229.
- Kalafat, D. (1989). Interpretation some of the great earthquake has occurred in the recent years in terms of focal mechanism. *Earthquake Research Bulletin*, 66, 6–33.
- Kalafat, D. (1998). Analyzed in terms of earthquake mechanisms of Anatolia tectonic structure. *Earthquake Research Bulletin*, 77, 1–217.
- Kalafat, D., Kekovalı, K., Güneş, Y., Yılmaz, M., Kara, M., Deniz, P., & Berberoğlu, M. (2009). *A catalogue of source parameters of moderate and strong earthquakes for Turkey and its surrounding area (1938–2008)* (pp. 1–43). İstanbul: Boğaziçi University Publication 1026.
- Karacık, Z., & Yılmaz, Y. (1998). Geology of the ignimbrites and the associated volcano–plutonic complex of the Ezine area, northwestern Anatolia. *Journal of Volcanology and Geothermal Research*, 85, 251–264.
- Kaymakçı, N., Aldanmaz, E., Langereis, C., Spell, T. L., Gürer, O. F., & Zanetti, K. A. (2007). Late Miocene transcurrent tectonics in NW Turkey: Evidence from palaeomagnetism and 40Ar–39Ar dating of alkaline volcanic rocks. *Geological Magazine*, 144, 379–392.
- Kaymakçı, N., White, S. H., & van Dijk, P. M. (2000). Paleostress inversion in a multiphase deformed area: Kinematic and structural evolution of the Çankırı Basin (central Turkey), part 1. In E. Bozkurt, J. A. Winchester, & J. A. D. Piper (Eds.), *Tectonics and magmatism in Turkey and the surrounding area* (pp. 445–473). London: Geological Society Special Publications 173.
- Koçyiğit, A. (1988). Tectonic setting of the Geyve Basin: Age and total displacement of the Geyve Fault Zone. In *1987 Melih Tokay symposium special published* (pp. 81–104). Ankara: Middle-East Technical University.
- Koçyiğit, A., Yılmaz, A., Adamia, S., & Kuloshvili, S. (2001). Neotectonics of East Anatolian Plateau (Turkey) and lesser Caucasus: Implication for transition from thrusting to strike-slip faulting. *Geodinamica Acta*, 14, 177–195.
- Koçyiğit, O. (2013). *Geç Antik Çağda Assos Konut Mimarlığı* [Assos residential architecture in the Late Antiquity] (PhD thesis, p. 320). Çanakkale Onsekiz Mart University, Turkey (in Turkish).
- Kozacı, Ö., Dolan, J. F., & Finkel, R. C. (2009). A late Holocene slip rate for the central North Anatolian fault, at Tah-taköprü, Turkey, from cosmogenic 10Be geochronology: Implications for fault loading and strain release rates. *Journal of Geophysical Research*, 114, 1–12.
- Kozacı, Ö., Dolan, J. F., Yönlü, Ö., & Hartleb, R. D. (2011). Paleoseismologic evidence for the relatively regular recurrence of infrequent, large-magnitude earthquakes on the eastern North Anatolian fault at Yaylabeli, Turkey. *Lithosphere*, 3, 37–54.
- Krantz, R. W. (1988). Multiple fault sets and three-dimensional strain: Theory and application. *Journal of Structural Geology*, 10, 225–237.
- Krushensky, R. (1976). Neogene calc-alkaline extrusive and intrusive rocks of the Karalar-Yeşiller area, Northwest Anatolia, Turkey. *Bulletin Volcanologique*, 40, 336–360.
- Krushensky, R., Akçay, Y., & Karaege, E. (1980). Geology of the Karalar-Yeşiller area, Northwest Anatolia. *Geological Survey Bulletin*, 1461, 1–72.

- Kürçer, A., Chatzipetros, A., Tutkun, S. Z., Pavlides, S., Ateş, Ö., & Valkaniotis, S. (2008). The Yenice-Gönen active fault (NW Turkey): Active tectonics and palaeoseismology. *Tectonophysics*, 453, 263–275.
- Le Pichon, X., Şengör, A. M. C., Demirbağ, E., Rangin, C., İmren, C., Armijo, R., ... Tok, B. (2001). The active Main Marmara fault. *Earth and Planetary Science Letters*, 192, 595–616.
- Lips, A. L. W. (1998). Temporal constraints on the kinematics of the destabilization of an orogen; syn-to post-orogenic extensional collapse of the northern Aegean region. *Geologica Ultraiectina*, 166, 1–224.
- Marrett, R., & Allmendinger, R. W. (1990). Kinematic analysis of fault-slip data. *Journal of Structural Geology*, 12, 973–986.
- McKenzie, D. (1972). Active tectonics of the Mediterranean region. *Geophysical Journal International*, 30, 109–185.
- McKenzie, D. (1978). Active tectonics of the Alpine-Himalayan belt: The Aegean Sea and surrounding regions. *Geophysical Journal International*, 55, 217–254.
- Metzger, R. (1994). *Geologie, Geochemie, Zirkonmorphologie und  $^{207}\text{Pb}/^{206}\text{Pb}$ -Datierung an Einzelzirkonen des Kazdag-Complexes (Biga-Halbinsel, NW-Türkei)* [Geology, geochemistry, zircon morphology and  $^{207}\text{Pb} / ^{206}\text{Pb}$  dating to single zircon from Kazdag-Complexes (Biga Peninsula, NW Turkey)] (PhD thesis, p. 80). Universität Tübingen.
- Okay, A. İ. (1987). *Biga Yarımadasının batı kesiminin jeolojisi ve tektoniği* [Geology and tectonics of the western part of the Biga Peninsula], (Raport No. 2374). İstanbul: İstanbul Technical University, Earth Science and Mineral Resources Center Publication.
- Okay, A. İ., Demirbağ, E., Kurt, H., Okay, N., & Kuşçu, İ. (1999). An active, deep marine strike-slip basin along the North Anatolian fault in Turkey. *Tectonics*, 18, 129–147.
- Okay, A. İ., & Göncüoğlu, C. (2004). The Karakaya Complex: A review of data and concepts. *Turkish Journal of Earth Sciences*, 13, 77–95.
- Okay, A. İ., & Satir, M. (2000). Coeval plutonism and metamorphism in a latest Oligocene metamorphic core complex in northwest Turkey. *Geological Magazine*, 137, 495–516.
- Okay, A. İ., Satir, M., Maluski, H., Siyako, M., Monie, P., Metzger, R., & Akyüz, S. (1996). Paleo- and Neo-Tethyan events in northwestern Turkey: Geologic and geochronologic constraints. In A. Yin & M. Harrison (Eds.), *Tectonics of Asia* (pp. 420–441). Cambridge: Cambridge University Press.
- Okay, A. İ., Satir, M., & Siebel, W. (2006). Pre-Alpide Paleozoic and Mesozoic orogenic events in the eastern Mediterranean region. In D. G. Gee & R. A. Stephenson (Eds.), *European lithosphere dynamics* (pp. 389–405). London: Geological Society 32.
- Okay, A. İ., Siyako, M., & Bürkan, K. A. (1991). Geology and tectonic evolution of the Biga Peninsula, Special Issue on Tectonics. *Bulletin of the Technical University of İstanbul*, 44, 191–256.
- Öcal, N. (1968). *Türkiyenin Sismisitesi ve Zelzele Coğrafyası, 1850–1960 Yılları İçin Zelzele Kataloğu* [Seismicity and earthquake geography in Turkey, earthquake catalogue for 1850–1960] (Vol. 8). İstanbul: Publications of Kandilli Observatory Publications (in Turkish).
- Özaksoy, V., Emre, Ö., Yıldırım, C., Doğan, A., Özalp, S., & Tokay, F. (2010). Sedimentary record of late Holocene seismicity and uplift of Hersek restraining bend along the North Anatolian Fault in the Gulf of İzmit. *Tectonophysics*, 487, 33–45.
- Özalp, S., Emre, Ö., & Doğan, A. (2013). The segment structure of southern branch of the North Anatolian Fault and paleoseismological behaviour of the Gemlik Fault, NW Anatolia. *General Directorate of Mineral Research and Exploration (MTA) Bulletin*, 147, 1–17.
- Papazachos, B., & Papazachou, C. (1997). *The earthquakes of Greece*. Thessaloniki-Greece: Editions Ziti.
- Philippson, A. (1910). *1/300.000 Geologische Karte des westlichen Kleinasien Blatt 1*. [1/300.000 scale Geological map of western Asia Minor (Part 1)]. Gotha: Justus Perthes.
- Pınar, N., & Lahn, E. (1952). *Turkish earthquake catalog with descriptions* (Technical Report, Serial 6, No. 36). Ankara: Turkey The Ministry of Public Works and Settlement, The General Directorate of Construction Affairs.
- Polat, G. (2002). Antandros. *İzmir Kent Kültürü Dergisi*, 5, 154–159.
- Polat, G. (2008). Antandros Nekropolü Ölü Gömme Gelenekleri [Antandros necropolis burial traditions]. *Anadolu Ek Dizi*, 2, 271–280 (in Turkish).
- Ramsey, C. B., & Lee, S. (2013). Recent and planned developments of the program OXCAL. *Radiocarbon*, 55, 720–730.
- Reimer, P. J., Bard, E., Bayliss, A., Beck, J. W., Blackwell, P. G., Ramsey, C. B., ... van der Plicht, J. (2013). IntCal13 and Marine13 radiocarbon age calibration curves 0–50,000 years cal BP. *Radiocarbon*, 55, 1869–1887.
- Republic of Turkey Prime Ministry Disaster & Emergency Management Presidency-Earthquake Research Department (AFAD-ERD). Retrieved from <https://www.afad.gov.tr/en/Index.aspx>.
- Rockwell, T., Barka, A., Dawson, T., Akyüz, S., & Thorup, K. (2001). Paleoseismology of the Gaziköy-Saros segment of the North Anatolia fault, northwestern Turkey: Comparison of the historical and paleoseismic records, implications of regional seismic hazard, and models of earthquake recurrence. *Journal of Seismology*, 5, 433–448.
- Rockwell, T., Ragona, D., Seitz, G., Langridge, R., Aksoy, M. E., Uçarkuş, G., ... Akbalık, B. (2009). Palaeoseismology of the North Anatolian Fault near the Marmara Sea: Implications for fault segmentation and seismic hazard. In K. Reicherter, A. M. Michetti, & P. G. Silva (Eds.), *Palaeoseismology: Historical and prehistorical records of earthquake ground effects for seismic hazard assessment* (pp. 31–54). London: Geological Society, Special Publication 316.
- Saka, K. (1979). *Edremit Körfezi ve civarı Neojeni'nin jeolojisi ve hidrokarbon olanakları* [The Neogene geology of Edremit bay and surrounding area and hydrocarbon facilities] (Turkey Petroleum Corporation Search Group Report 1341, 17 p.) (in Turkish).
- Schuling, R. D. (1959). Über eine pra-herzynische faltungsphase im Kaz-Dağ kristallin [About a Pre-Hercinian folding in Kazdağ crystalline complex]. *Journal of Mineral Research and Exploration Institute of Turkey*, 53, 89–93 (in German).
- Şengör, A. M. C. (1979). The North Anatolian transform fault: Its age, offset and tectonic significance. *Journal of the Geological Society London*, 136, 269–282.
- Şengör, A. M. C., Görür, N., & Şaroğlu, F. (1985). Strike-slip faulting and related basin formation in zones of tectonic escape: Turkey as a case study. In K. T. Biddle & N. Christie-Black (Eds.), *Strike-slip deformation, basin formation and sedimentation* (pp. 227–264). Society of Economic Mineralogist and Paleontologists, Special Publication No. 37. Tulsa: USA.
- Şengör, A. M. C., Grall, C., İmren, C., Le Pichon, X., Görür, N., Henry, P., ... Siyako, M. (2014). The geometry of the North Anatolian transform fault in the Sea of Marmara and its temporal evolution: Implications for the development of intracontinental transform faults. *Canadian Journal of Earth Sciences*, 51, 222–242.
- Şengör, A. M. C., Tüysüz, O., İmren, C., Sakıncı, M., Eyidoğan, H., Görür, G., & Le Pichon, X. (2005). The

- North Anatolian Fault: A new look. *Annual Review of Earth and Planetary Sciences*, 33, 37–112.
- Serdaroğlu, Ü. (1996). *Behramkale Assos*, İstanbul: Archaeology & Art Publications. ISBN: 9789757538752.
- Shebalin, N. V., Karnik, V., & Hadzievski, D. (1974). *Catalogue of earthquakes*. Skopje-Yugoslavia: UNESCO.
- Siyako, M., Bürkan, K. A., & Okay, A. İ. (1989). Biga ve Gelibolu Yarımadalarının Tersiyer jeolojisi ve hidrokarbon olanakları [Tertiary geology of Biga and Gelibolu Peninsula and their hydrocarbon facilities]. *Turkish Association of Petroleum Geologists Bulletin*, 1/3, 183–199.
- Soloviev, S. L., Solovieva, O. N., Go, C. N., Kim, K. S., & Shchetnikov, N. A. (2000). *Tsunamis in the Mediterranean Sea, 2100 B.C.–2000 A.D.* Dordrecht: Kluwer Academic Publishers.
- Soysal, H., Sipahioğlu, S., Kolçak, D., & Altınok, Y. (1981). *Historical earthquake catalogue of Turkey and surrounding area (2100 B.C.–1900 A.D.)* (Technical Report, TUBİTAK, No: TBAG-341).
- Sperner, B., Muller, B., Heidebach, O., Delvaux, D., Reinecker, J., & Fuchs, K. (2003). Tectonic stress in the Earth's crust: Advances in the World Stress Map project. In D. A. Nieuwland (Ed.), *New insight into structural interpretation and modelling* (pp. 101–116). London: Geological Society of London Special Publication No. 212.
- Sperner, B., & Zweigel, P. (2010). A plea for more caution in fault-slip analysis. *Tectonophysics*, 482, 29–41.
- Suzanne, P., Lyberis, N., Chorowicz, J., Nurlu, M., Yürür, T., & Kasapoğlu, E. (1990). La géométrie de la faille nord anatolienne a partir d'images Landsat-MSS [The geometry of the North Anatolian fault from Landsat-MSS images]. *Bulletin de la Societe Geologique de France*, VI, 589–599.
- Tan, O., & Taymaz, T. (2004). Seismotectonics of the Caucasus and surrounding regions: Source parameters and rupture histories of recent destructive earthquakes. *AGU Fall Meeting, EOS Transactions*, 85 (47), Session T14, San Francisco-California.
- Taymaz, T. (1999, August 17). Seismotectonics of the Marmara Region: Source characteristics of 1999 Gölcük – Sapanca – Düzce earthquakes. In *Proceedings of ITU-LAHS, International Conference on the Kocaeli Earthquake*, İstanbul. (pp. 55–78).
- Tibi, R., Bock, G., Xia, Y., Baumbach, M., Grosser, H., Milkereit, C., ... Zschau, J. (2001). Rupture processes of the 1999 August 17 Izmit and November 12 Düzce (Turkey) earthquakes. *Geophysical Journal International*, 144, F1–F7.
- United States Geological Survey National Earthquake Information Center (USGS-NEIC). Retrieved from <http://earthquake.usgs.gov/contactus/golden/neic.php>
- Vandycke, S., & Bergerat, F. (2001). Brittle tectonic structures and palaeostress analysis in the Isle of Wight, Wessex basin, southern U.K. *Journal of Structural Geology*, 23, 393–406.
- van der Kaaden, G. (1959). Anadolunun Kuzeybatı Kısımında Yer Alan Metamorfik Olaylarla Magmatik Faaliyetler Arasındaki Yaş Münasebetleri [The metamorphic events between magmatic activities and their age relations in the northwestern part of Anatolia]. *MTA Dergisi*, 52, 15–34 (in Turkish).
- Will, T. M., & Powell, R. (1991). A robust approach to the calculation of paleostress fields from fault plane data. *Journal of Structural Geology*, 13, 813–821.
- Yalıtırak, C. (2003). *Edremit Körfezi ve Kuzeyinin Jeodinamik Evrimi* [Geodynamic evolution of the Gulf of Edremit and its North] (PhD thesis, p. 245). İstanbul: İstanbul Technical University, Institute of Avrasya Earth Sciences.
- Yalıtırak, C. (2006). Kazdağı'nın Tektonik Yapısı ve Edremit Körfezi'ni Karadan Sınırlayan Fayların Karakterleri [The tectonic structure of Kazdağı and character of faults bounding Edremit Bay from land]. *ATAG-10 Bildiri Özleri Kitabı* 94–95 (in Turkish).
- Yalıtırak, C., & Okay, A. İ. (2004). Geology of the Paleotetis units at the northern part of Edremit Bay. *Journal of Istanbul Technical University*, 3, 67–79.
- Yamaji, A. (2000). The multiple inverse method: A new technique to separate stresses from heterogeneous fault-slip data. *Journal of Structural Geology*, 22, 441–452.
- Yılmaz, Y., & Karacık, Z. (2001). Geology of the northern side of the Gulf of Edremit and its tectonic significance for the development of the Aegean grabens. *Geodinamica Acta*, 14, 31–43.
- Yin, Z. M., & Ranalli, G. (1993). Determination of tectonic stress field from fault slip data: Toward a probabilistic model. *Journal of Geophysical Research: Solid Earth*, 98, 12165–12176.
- Yoshioka, T., & Kuşçu, İ. (1994). Late Holocene faulting events on the İznik-Mekece fault in the western part of the North Anatolian Fault Zone, Turkey. *Bulletin of the Geological Survey of Japan*, 45, 677–685.
- Žalohar, J., & Vrabec, M. (2007). Paleostress analysis of heterogeneous fault-slip data: The Gauss method. *Journal of Structural Geology*, 29, 1798–1810.
- Zimmermann, F. (1945). *6.10.1944 tarihinde vuku bulan Ayvacık-Ayvalık yersarsıntısı* [Ayvacık-Ayvalık Earthquake occurred on October 6, 1944] (Report No. 025.343 Dab0) Ankara: Earthquake Research Centre Pub.